

Super-Resolution Structured Illumination Microscopy

Rainer Heintzmann^{*,†,‡} and Thomas Huser^{*,§,||,¶}

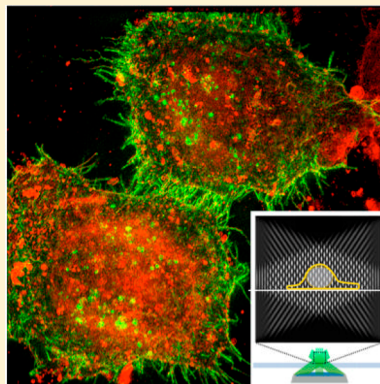
[†]Leibniz Institute of Photonic Technology, Albert-Einstein Straße 9, 07745 Jena, Germany

[‡]Institute of Physical Chemistry and Abbe Center of Photonics, Friedrich-Schiller-University Jena, 07745 Jena, Germany

[§]Biomolecular Photonics, Department of Physics, University of Bielefeld, Universitätsstraße 25, 33615 Bielefeld, Germany

^{||}Department of Internal Medicine and NSF Center for Biophotonics, University of California, Davis, Sacramento, California 95817, United States

ABSTRACT: Super-resolved structured illumination microscopy (SR-SIM) is among the most rapidly growing fluorescence microscopy techniques that can surpass the optical diffraction limit. The strength of SR-SIM is that it can be readily applied to samples prepared for conventional fluorescence microscopy, requiring no sophisticated sample preparation protocols. As an extension of wide-field fluorescence microscopy, it is inherently capable of multicolor imaging and optical sectioning and, with sufficiently fast implementations, permits live cell imaging. Image reconstruction, however, currently relies on sophisticated computational procedures, susceptible to reconstruction artifacts, requiring trained users to recognize and avoid them. Here, we review the latest developments in SR-SIM research. Starting from a historical overview of the development of SR-SIM, we review how this method can be implemented in various experimental schemes, we provide an overview of the important parameters involved in successful image reconstruction, we summarize recent biological applications, and we provide a brief outlook of the directions in which we believe SR-SIM is headed in the future.



CONTENTS

1. Introduction	13890
2. The Origins of SR-SIM	13891
3. The Nitty-Gritty Details of Realizing SR-SIM	13892
4. Labeling Strategies for SR-SIM	13893
5. Reconstruction Algorithms for SR-SIM	13895
5.1. The Nitty-Gritty Details of SIM Image Reconstruction	13896
5.2. The Complications of 3D-SIM	13898
5.3. BlindSIM Image Reconstruction	13898
5.4. Avoiding SR-SIM Image Reconstruction Artifacts	13900
6. Alternative Approaches to SR-SIM	13900
7. Combining SR-SIM with Other Super-Resolution Modalities	13901
8. Increasing the Resolution beyond a Factor of 2: Nonlinear SR-SIM	13901
9. Applications of SR-SIM to Cell Biology	13902
10. Conclusions and Perspective	13904
Associated Content	13904
Special Issue Paper	13904
Author Information	13904
Corresponding Authors	13904
ORCID	13904
Notes	13904
Biographies	13904
Acknowledgments	13905
References	13905

1. INTRODUCTION

Super-resolved structured illumination microscopy (SR-SIM) is one of the most universally implemented optical super-resolution techniques, applicable to a wide variety of biological problems. The main charm of SR-SIM lies in the fact that it can readily be applied to samples that are prepared for standard fluorescence microscopy without requiring significant additional sample preparation effort. In addition, SR-SIM is multicolor capable: typically demonstrated and implemented in up to four different color channels. It places no special requirements on the fluorophores used for sample labeling other than that they have to be reasonably resistant to photobleaching. Since structured illumination microscopy was first demonstrated around the same time as stimulated emission depletion (STED) microscopy, it can be counted among the original super-resolution microscopy techniques, having been implemented through a wide range of schemes.^{1,2} Because of this, a number of terms that describe its different implementations, such as two-dimensional SIM (2D-SIM), three-dimensional SIM (3D-SIM), total internal reflection fluorescence SIM (TIRF-SIM), coherent SIM, standing wave illumination, etc., can be found in the literature. While we will briefly describe the differences between these different implementations in this review, we will primarily use the term SR-SIM to refer to the basic technique utilizing a periodic

Received: April 26, 2017

Published: November 10, 2017

interference pattern with a periodicity near the optical diffraction limit, in order to distinguish it from an even older method, also called SIM, that uses comparably coarse structured illumination patterns to obtain depth profiles of macroscopic objects³ or to achieve optical sectioning.⁴

One of the main qualities of SR-SIM is its extremely efficient use of the available photon budget. As a wide-field imaging technique that can utilize the latest generation of highly sensitive imaging cameras, it collects and detects fluorescence photons with the highest possible efficiency, while also minimizing the amount of excitation power needed to excite fluorescence. This quality, combined with the high imaging speed that this facilitates, also makes SR-SIM one of the most suitable techniques for live cell imaging. Although SR-SIM is, in its original implementation, limited to a factor of approximately 2 in improving the spatial resolution, this barrier can also be superseded with somewhat more sophisticated optical schemes or more fundamentally by exploiting a nonlinear sample response. In this review, we aim to summarize the developments that lead up to the current state-of-the-art in SR-SIM, we describe the different forms in which this method has been implemented, we list typical pitfalls and how they can be avoided, we discuss image reconstruction methods, we compare SR-SIM with recent similar developments based on confocal optics, and we review some of the latest applications of SR-SIM in biological imaging.

2. THE ORIGINS OF SR-SIM

The use of periodic illumination patterns (also known as “structured illumination”) is a long-existing methodology that was originally used for surface profiling³ and similar applications or as a depth discrimination method to reject out-of-focus contributions from different vertical image planes.⁴ As structured illumination microscopy (SIM) in its current form aims at improving the lateral and axial resolution of fluorescence microscopy, it is instructive to look at early work aimed at improving the optical resolution. Especially noteworthy in this context is the work of Lukosz^{5,6} in the late 1960s. Lukosz et al. placed a coding illumination structure (stripes⁷ or 2D patterns⁶) directly (without the use of lenses) in front of the object to image. They then decoded the patterns by application of a matching structure in the conjugate image plane, which was translated relative to the scanned sample. In a beautiful derivation that bears striking similarities to present-day super-resolution SIM image processing, it is explained why such a Nipkow-disk-like setup leads to an effective increase of the detection passband compared to head-on low numerical aperture (NA) illumination. This work already utilized the Fourier-space description of the situation even though in these setups no individual images were acquired. The technique as described by Lukosz is closely related to synthetic aperture radar, which uses the knowledge of the phase of a moving radar antenna to improve the spatial resolution of radar systems. Compared to present-day SR-SIM, however, there is an important fundamental difference: Transmission SIM based on an elastically scattered (coherent) signal, for fundamental physical reasons, cannot achieve super-resolution beyond Abbe's far field limit considering both illumination and detection.⁸

This situation changes, however, fundamentally for incoherent emission such as fluorescence or spontaneous Raman scattering: In this case, the emitted light “forgets” information about the illumination phase, ensuring that the concept of

convolution with an intensity point spread function can be used as a simple description of imaging. This incoherent sample response (i.e., fluorescence) is the fundamental reason for SR-SIM's ability to achieve a spatial resolution corresponding to the sum of the maximum spatial frequencies (in excitation and emission) that can be transmitted through the optical system.

In the field of fluorescence, the excitation of fluorophores by a structured illumination pattern was used early on to achieve confocal-like optical sectioning.⁴ However, the relatively coarse illumination pattern and the algorithms used for this purpose (not requiring knowledge of the illumination phase) were unsuitable to achieve a substantial lateral resolution improvement compared to wide-field imaging with uniform illumination. The concept of standing wave microscopy promoted by Lanni and co-workers described a setup aimed at substantially increasing the axial resolution with the help of an axial sinusoidal illumination pattern generated by interfering opposing beams from the same laser.⁹ This approach, unfortunately, had a transfer function that left a substantial gap in the axial spatial frequencies and was therefore unsuitable for high-resolution imaging. This shortcoming was fixed by the I⁵M approach introduced by Gustafsson et al., which generates a short-range axial interference pattern using spatially and temporally incoherent illumination resulting in an axial resolution of approximately 100 nm.¹⁰ Even though this setup can be considered to be an axial form of structured illumination, it is in a way simpler than current SR-SIM: One acquired image stack in a well-adjusted system can be described as the sample having been convolved with one three-dimensional optical intensity transfer function. The illumination pattern is generated by the same objective lenses used for imaging. Moving the object between the two opposing objective lenses leads to the axial modulation looking like part of the point spread function, which simplifies the reconstruction substantially. In the case of lateral modulation of the illumination, the resulting images look as if the lateral illumination structure had been imprinted onto the sample in every image. In order to reconstruct a high resolution image, several images at different illumination phases have to be acquired to illuminate all parts of the sample, and to then unmix the overlapping Fourier components that encode the high resolution information. Such concepts of phase stepping are generally also well-known from coherent holography and have even been conceptualized for use in fluorescence by Lanni et al.⁹ In a patent by Ben-Levy it is conceptually described how such an unmixing approach can be used together with a lateral sinusoidal illumination to achieve a lateral resolution improvement.¹¹ The independently developed laterally modulated excitation microscopy, presented orally in 1998 at the SPIE Europe conference and published shortly thereafter,¹ was to our knowledge the first experimental demonstration of such a concept demonstrating SR-SIM for the fluorescence case. The unmixing mathematics of this publication still lacked the matrix notation and the weighted averaging step had not yet been introduced.

Gustafsson improved upon this approach in a seminal publication in 2000² where the reconstruction mathematics contained the matrix description (see also ref 12) and the weighted averaging approach that makes SR-SIM particularly powerful. His publication was also the first to experimentally verify the factor of 2 in bandwidth extension (i.e., resolution increase). So et al.¹³ then published a SR-SIM-like method using total internal reflection (TIR) for illumination, which

further increased the achievable bandwidth. Using TIR illumination launched by an external prism, Frohn et al.¹⁴ were able to show a resolution of 100 nm by standing wave illumination. In 2003, two-dimensional structured illumination with unmixing and an interesting concept to reduce the required minimum number of images with different illumination phases was presented.¹⁵

The Stemmer group later followed the conceptual presentation of SIM useful for three-dimensional resolution enhancement¹⁶ by publishing a conceptual paper on three-beam SR-SIM.¹⁷ A very impressive combination of lateral and axial illumination structuring (I³S) was presented by Gustafsson in 2008.¹⁸ Significant advances in the reconstruction approaches and imaging speed were then made over the following years.^{19–22}

Linear structured illumination for fluorescence microscopy improves the resolution essentially by separating spatially structured illumination and spatially resolved detection, and by exploiting the loss of phase relationship (incoherence) between emitters. This leads to the mathematical addition of the (Abbe) frequency limits for excitation and detection. However, by using the sample as a means to distort the linear response between incoming and emitted light, the extraction of higher harmonics can break this factor-of-2 limit. Nonlinear sample responses have been known to achieve super-resolution and form the fundamental basis for super-resolution beyond twice the Abbe limit.^{15,23} Even though many of the nonlinear approaches yield fundamentally unlimited resolution, the type and strength of nonlinearity will define which resolution is practically achievable for signal-to-noise reasons. Multilinear superposition and saturation effects that occur during switching between molecular states and light-induced changes of the emission ability along with exploiting quantum mechanical coherence in Rabi oscillations have been suggested as possible nonlinear mechanisms useful for extending SIM beyond doubled spatial resolution.²⁴ Such nonlinear effects are essentially also exploited in STED,^{25,26} and the nonlinearity in photoinduced switching²⁴ is exploited in RESOLFT (reversible saturable optical fluorescence transitions).²⁷ The general concept that a nonlinear sample response leads to a resolution fundamentally beyond Abbe's limit has been around longer than any specific realizations in fluorescence.²⁸

3. THE NITTY-GRITTY DETAILS OF REALIZING SR-SIM

To fully exploit the potential for increased spatial resolution of SR-SIM, it is imperative that mutually coherent beams are brought to interference to generate the highest modulation frequency, and the highest contrast for the laser excitation pattern. This requirement, however, necessitates certain rules that have to be kept in mind when designing different optical excitation paths for SR-SIM. First, one needs to decide if 2D or 3D mode of operation is desired. Most of the early adopters chose to implement two-beam total internal reflection fluorescence (TIRF) excitation, which is facilitated by generating a standing wave pattern above the glass surface by allowing two laser beams (split from a single source) to interfere at angles beyond the angle of total internal reflection. Initially, this was implemented by generating the standing wave pattern above a glass prism and imaging the fluorescence with a separate microscope objective lens.^{13,14,29,30} In more recent implementations, this condition can also be met by utilizing TIRF through microscope objective lenses with a numerical aperture exceeding 1.4.^{31,32} This mode of illumination and the

resulting excitation pattern are shown schematically in Figure 1a. In order to successfully reconstruct images in this 2D

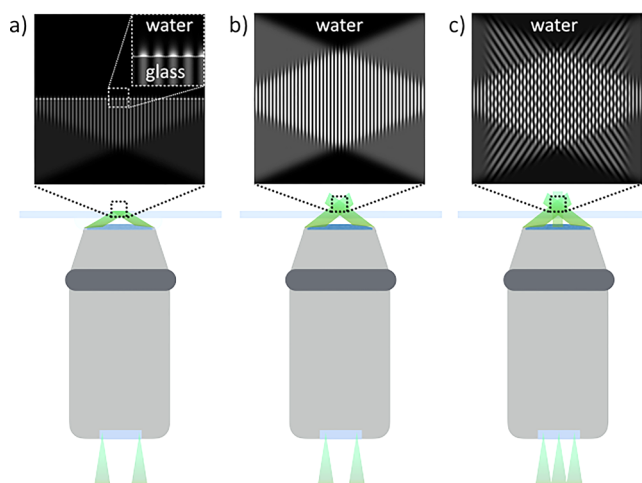


Figure 1. Schematics of different illumination modes in structured illumination microscopy (SIM). The beams at the rear side of the microscope objective lens are shown relative to the back aperture, limiting the acceptance angle of the back focal plane. For oil-immersion objective lenses with numerical apertures exceeding NA 1.4, relaying the beams to the maximum position off the optical axis leads to total internal reflection at the upper side of the glass coverslip; two-beam illumination results in counterpropagating evanescent waves, penetrating <100 nm into the sample (TIRF-SIM) (a). Two-beam interferences create a 2D interference pattern in the sample (two-beam SIM) (b), and adding a central beam leads to a 3D interference pattern (three-beam SIM) (c).

implementation, a mostly isotropic resolution along the lateral directions is desired. To fulfill this requirement to some extent, it has become customary to utilize illumination along three angles with three phase steps per angle, resulting in nine raw images that are ultimately assembled into a single reconstructed SR-SIM image. The TIRF condition is, however, not strictly needed to generate 2D interference patterns, and is often not desired, because it restricts the excitation light to a very narrow region (approximately 100–200 nm) above the glass surface. This limits the choice of biological problems that can be studied by this approach to processes that occur near the cellular plasma membrane. Alternatively, two-beam interference can also be achieved for excitation beams that are routed into the microscope objective lens at angles below the angle of total internal reflection.¹⁶ This is demonstrated schematically in Figure 1b. In this case, a larger volume within the cell is illuminated, leading to reduced spatial resolution and often undesired background (out-of-focus) contributions along the axial direction, but several approaches to managing these problems have been described as we will briefly discuss in section 5. Three-beam illumination, which also utilizes a central beam in addition to the two off-axis beams, results in a true three-dimensional excitation pattern as shown schematically in Figure 1c.

At this point it should be mentioned that, in order to achieve the highest possible modulation depth, the polarization of the interfering laser beams has to be kept parallel to the stripe direction. In the standing wave approach, this condition can easily be met, whereas for two-beam (and three-beam) illumination through a microscopy objective lens, this requires dynamic adjustments of the polarization, either through fast,

electrooptical (e.g., liquid-crystal based) devices, or, in a more static solution, by designing and utilizing segmented wave plates oriented at the appropriate angles for the different excitation angles. Furthermore, for three-beam SIM, in order to ensure similar contrast ratios along the vertical direction for all horizontal patterns, circularly polarized light is used for the central beam. The static solution does, however, pose an additional concern for multicolor operation since some wave plates perform only well for their design wavelength.

This brings us to the question of how the different, interfering laser beams and the different angles (and phases) at which they interfere can most flexibly be generated. In the original three-beam demonstration for cellular imaging, Gustafsson et al. chose a diffraction grating to split a laser beam into different diffraction orders and they utilized the zero diffraction order as the central beam, as well as the +1 and -1 diffraction orders for the angular beams.³³ In this case, modifying the excitation pattern could be most easily achieved by physically rotating the diffraction grating and shifting it along the grating direction by a piezo translation stage. This approach works well in producing the different angles and phases, but the mechanical manipulation of the diffraction grating is time-consuming, which pretty much prohibits any live cell imaging application. Thus, more recent generations have utilized electrooptic devices, such as spatial light modulators to flexibly generate diffraction gratings with different angles and phase shifts. Other methods, such as the use of acoustooptic deflectors³⁴ or digital mirror devices,³⁵ have also been demonstrated.

In impressive extensions, the original SIM approach has recently also been utilized in light-sheet illumination as implemented in lattice light-sheet illumination³⁶ and by generating standing wave patterns through counterpropagating light sheets.^{37,38} Although this does not take advantage of the interference approach, SIM reconstruction methods can also improve the spatial resolution of two-photon microscopy by Bessel beam illumination.³⁹ These implementations, to some extent, have also helped to alleviate a problem with the limited penetration depth, which, due to the optical aberrations encountered in wide-field illumination, has so far limited SR-SIM to about 15 μm imaging depth in the vertical direction, reaching up to 30 μm depth in exceptional cases.

Another important point that cannot be neglected is that SR-SIM requires careful characterization of the point spread function (PSF) of the microscope or, in terms of its Fourier transform, which is utilized in the reconstruction process, the optical transfer function (OTF) of the microscope. For 2D implementations of SR-SIM, a theoretical PSF which can be calculated from some of the basic optical parameters of the system (excitation/emission wavelength, NA of the objective lens, etc.) can be used to approximate the experimental PSF, but especially for 3D implementations, an experimental PSF should be acquired. This is typically achieved by imaging a robust point source, such as a 100 nm fluorescent polymer bead. During this process, as well as throughout the entire imaging process, it is imperative to minimize sample drift, mechanical drift of the microscope itself, and vibrations, because all of these will reduce the chances of obtaining meaningful reconstructed SR-SIM images with minimal artifacts. As a wide-field imaging technique, SR-SIM is particularly prone to imaging artifacts. Typical optical artifacts are caused by chromatic aberrations in multicolor operation, as well as spherical aberration. Spherical aberration can be reduced

or worsened depending on the mismatch between the index of refraction between the microscope objective lens, the immersion medium, and the substrate on which the sample has been prepared and is easily recognized as a violation of the axial symmetry of the PSF. Adjusting the index of refraction of the immersion oil can be used to minimize spherical aberrations. Alternatively, some research groups have begun to combine adaptive optics with SR-SIM in order to reduce aberrations and to increase imaging depth.^{40,41}

Photobleaching of the sample during continued exposure results in a continuous reduction of the signal-to-noise ratio, which makes image reconstruction artifacts become more significant for later frames acquired in a time-lapse series. The sequence in which SR-SIM raw data are acquired can also add to this effect; e.g., if in 3D-SIM an entire vertical stack is first acquired for one angle, before rotating the angle to the next position, this will result in photobleaching during acquisition at the initial angle setting, which will cause a lower signal-to-noise ratio in the raw data images acquired for the angles that are acquired later in the series.

4. LABELING STRATEGIES FOR SR-SIM

Among the biggest advantages of SR-SIM is that it places no special requirements on the (fluorescent) probes that are used for imaging, other than that they need to be fairly resistant to photobleaching and, ideally, nonblinking. Because of this, a wide range of organic and genetically expressible fluorophores work well for SR-SIM and have already been widely applied to biological problems. Other probes, such as fluorescent semiconductor quantum dots,⁴² nanodiamonds containing fluorescent nitrogen vacancies,⁴³ fluorescent silica or polymer beads, upconverting nanoparticles,⁴⁴ and also water-soluble conjugated polymers,⁴⁵ are quite well-suited for SR-SIM and will further open it up to applications in chemistry and materials science. Recently, even other sources of incoherent photons, such as gold and silver nanoparticles capable of surface-enhanced Raman scattering, have been demonstrated to provide excellent contrast for SR-SIM imaging.⁴⁶

The main applications are, however, found in the biological sciences, where initially fixed cellular structures and, more recently, even living cells have been imaged by SR-SIM. For fixed cell imaging, one can choose from the widest selection of fluorophores that are either initially expressed by the cells themselves, or added after fixation to specifically stain cellular structures of interest by immunofluorescence or other mechanisms of specific molecular binding. In this regard, it seems timely to add a word of caution for potential newcomers to super-resolution optical microscopy. As we are more or less approaching spatial resolutions on the 50 nm length scale, care needs to be taken with regard to the fixative. Paraformaldehyde in concentrations of 1–4% is often used to fix cells, but, as has been observed by electron and X-ray microscopies, this fixative leads to destructive effects on proteins and protein complexes resulting in artifacts on the tens of nanometers length scale.⁴⁷ These effects might not yet be obvious with the doubled resolution obtained by linear SR-SIM, but will become increasingly detrimental as the spatial resolution continues to be pushed. Other choices, such as glutaraldehyde fixation or cold methanol fixation, will have to be considered and compared to this traditional choice, albeit in many cases these perform worse. Another source of potential artifacts on these length scales are the artificially enlarged structures created by fluorescently labeled secondary antibodies which are

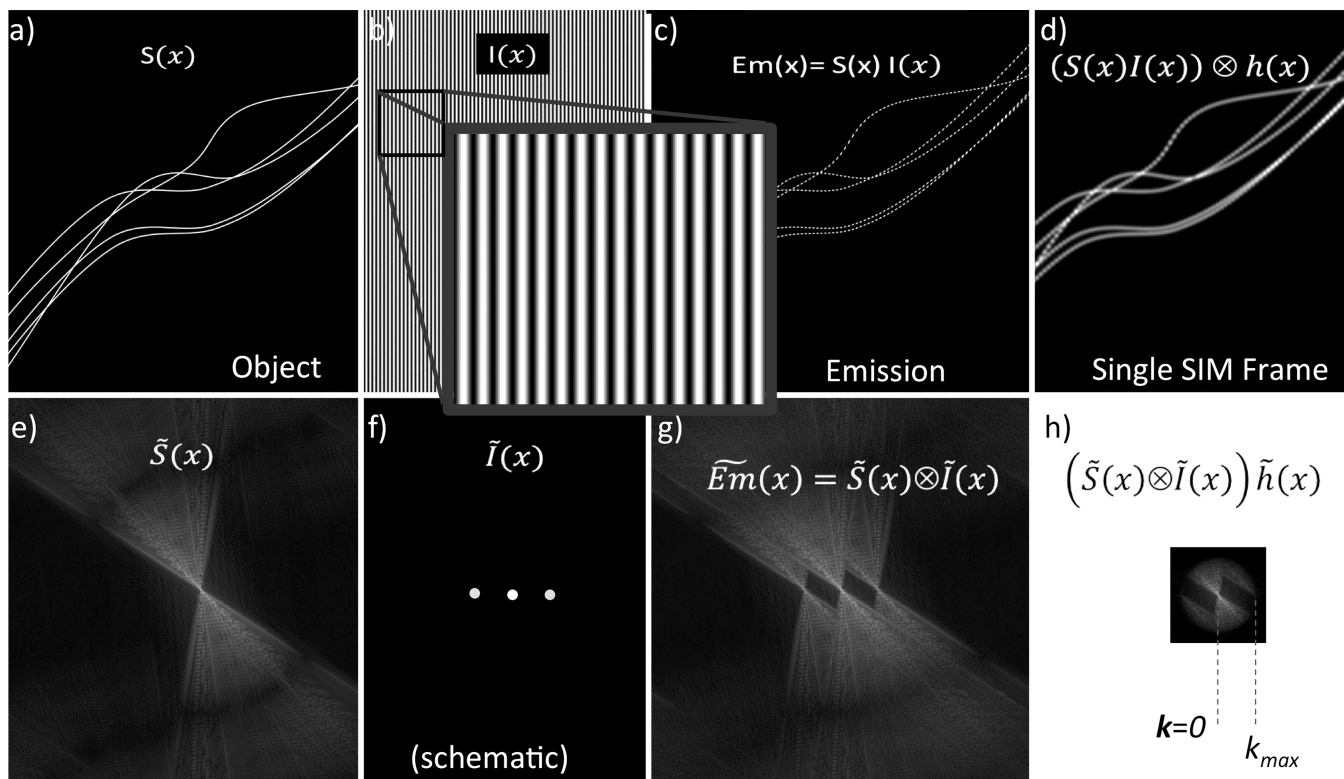


Figure 2. Model of two-beam SIM imaging. The object (a) is illuminated with a pattern (b) yielding an emission (c) which is blurred by the point spread function (d). Panels e–h show the corresponding operations in Fourier space. Note that only the information up to the wide-field Abbe limit k_{\max} is captured (panel h). For clarity purposes, these simulations do not include noise. The absolute magnitude of Fourier space images to the power of 0.3 is shown.

directed against primary antibodies. Lastly, the choice of embedding media which are often used to preserve samples and to minimize photobleaching can also affect sample integrity on these length scales. Hard-set media, such as the popular Prolong Gold and similar choices, have been shown to compress cells—most prominently in the axial direction—leading to deformations that are not observed in soft-set mounting media, such as Vectashield, Mowiol, or glycerol. These potential problems and pros and cons of sample preparation vs sample longevity need to be considered and probably compared before reporting novel observations in structural biology.

Once these initial sample preparation steps have been figured out, a wide choice of brightly fluorescent dyes are available for SR-SIM. Most modern, bleaching resistant fluorophores, e.g., rhodamine- and oxazine-derived organic fluorophores (e.g., the Alexa series of fluorophores from ThermoFisher or the Atto series from Atto-Tec) work well for SR-SIM. Biologists should, however, stay away from fluorescein, in particular the popular fluorescein isothiocyanate (FITC), which bleaches very rapidly. The most prominent fluorescent proteins, i.e., eGFP, mCherry, or Cerulean, work well, while we found YFP to be a poor choice because it photobleaches too quickly. Here, as is often the case, it is worthwhile to spend some time on evaluating a range of alternative fluorescent proteins for each specific problem. Fixed cell staining will, of course, also work well with other probes, such as the previously mentioned semiconductor quantum dots. Notably, prominent blinking, as often exploited in single molecule localization imaging experiments, which is caused by the photophysical properties of the dyes and the environment, should be avoided as much as possible in SIM.

Most of the fluorescent proteins will work just as well for living cells as they do in the fixed cell case, if the pH value is controlled well. Here, however, a number of other, cell-diffusible and cell-direct organic fluorophores are also often used. In our experience, prominent live cell stains, such as MitoTracker, ER-Tracker, or Lysotracker, all work well for imaging by SR-SIM, but as always, their red fluorescent versions are preferred in order to maximize their signal against the omnipresent cellular autofluorescence. Similarly, membrane stains are often used to either highlight all cells or specifically stain cellular subpopulations. The wide variety of available stains makes this choice rather cumbersome. Specifically for membrane stains of living cells we found that these should be used with great care. A membrane stain that works well for one type of cell might interfere with processes of interest in other cells. As an example, a stain that has become one of our favorites for membrane staining, CellMask Orange (or its DeepRed variation), worked well for staining T cells and enabled us to follow the transmission of HIV between T cells,⁴⁸ while the same stain had a rather detrimental effect on primary liver endothelial cells, rendering the cells immobile and making them very photosensitive. Instead, we found that DiO is a suitable stain for these primary cells, but it also photobleaches rather quickly. Depending on the specific problem of interest, it might be beneficial to utilize immunofluorescent probes against membrane proteins. Similarly, bleaching-resistant organic fluorescent probes that specifically stain internal structures of cells can often be incorporated into cells by gentle application of transfection agents, microinjection, or electroporation. Lately, in particular to enable nonlinear SIM or combinations of SR-SIM with other super-resolution methods, such as

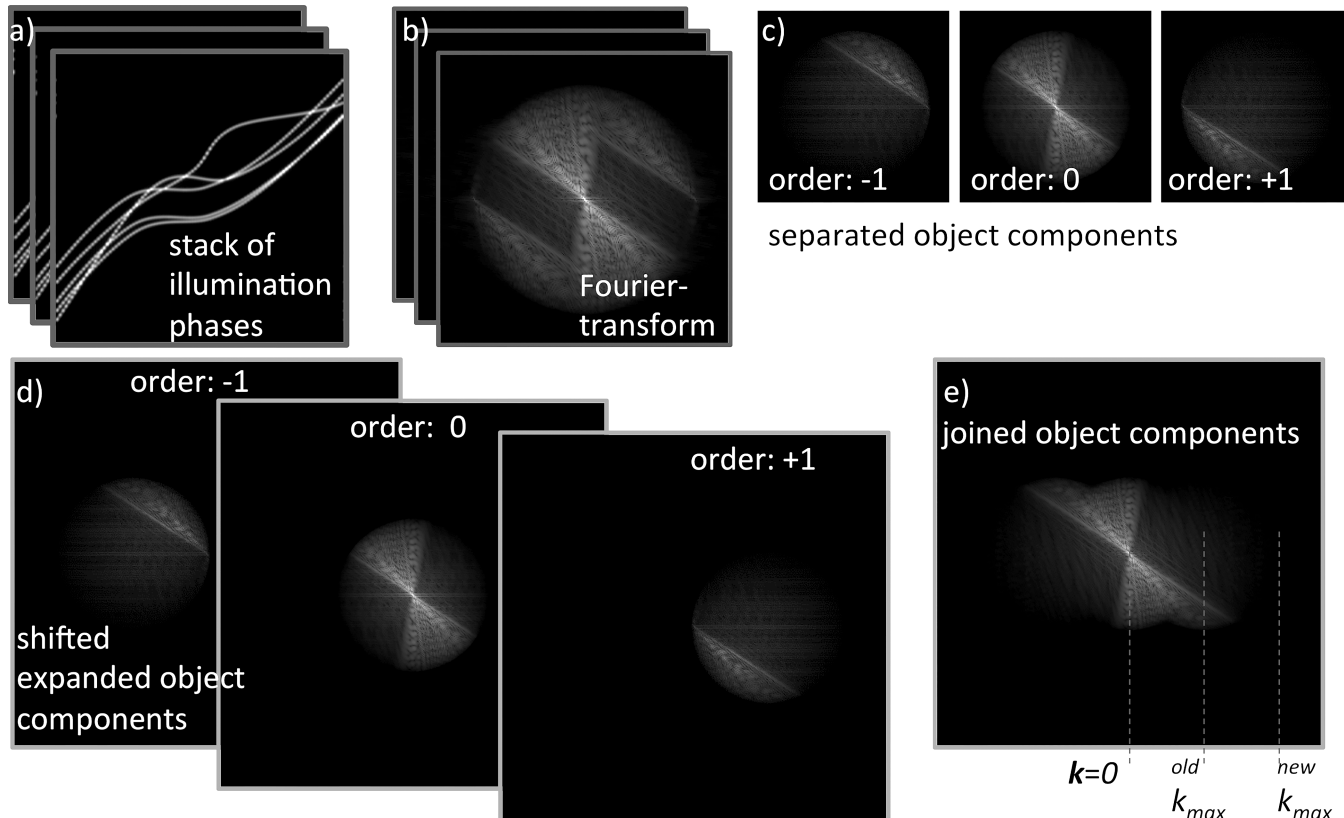


Figure 3. Schematics of SIM image reconstruction along one dimension. A series of images at different illumination phases (a) is Fourier transformed (b) and the components are separated (c). They are then shifted to their correct positions in k -space (d) and joined by weighted averaging (e).

PALM/STORM, photoswitchable fluorescent proteins, such as Dronpa,⁴⁹ mEos2, Skylan NS,⁵⁰ RS-eGFP, IRIS-FP, and Kohinoor,⁵¹ are also becoming increasingly popular choices to enable NL-SIM with a resolution down to about 50 nm.

5. RECONSTRUCTION ALGORITHMS FOR SR-SIM

Figure 2 describes the physical model explaining the process of linear SIM imaging. The fluorescence density $S(x)$ of the unknown sample (Figure 2a) is multiplied with the excitation intensity $I(x)$ (Figure 2b) in each location (x) to yield the local emission intensity $E_m(x)$ (Figure 2c), which is subsequently imaged by the microscope (Figure 2d), as described by the convolution with the detection point spread function $h(x)$. To understand the reconstruction process and the origin of the resolution enhancement, it is instructive to picture this same model in Fourier space as shown in Figure 2e–h. The multiplication of the illumination pattern with the sample structure in real space turns into a convolution to describe the Fourier transformed emission, generating an overlap of shifted object components. For the case of three-beam SIM the illumination intensity structure has seven delta peaks in Fourier space, where two pairs share the same lateral spatial frequency k_{xy} , respectively. This leads to the lateral emission light in Fourier space being described by five overlapping (summed) shifted copies of the object structure \tilde{S}_p , with “~” denoting the Fourier transform. To keep it simple, Figure 2 shows the case for two-beam SIM, corresponding to three overlapping orders in Fourier space. This Fourier-shifted object information contains all the information leading to the resolution improvement in SIM. As the emission has to undergo imaging,

i.e., a multiplication with the transfer function \tilde{h} in Fourier space, the trick is that this Fourier-shifted object information brings previously inaccessible information from outside the passband of the microscope (where \tilde{h} is zero) into the passband prior to imaging. The task of SIM image reconstruction therefore is to disentangle the overlapping object components and place them back in their correct positions in Fourier space leading to an overall extended transferred bandwidth of the system.

The principle of SIM reconstruction is shown in Figure 3. The overlapping components can be disentangled by ensuring that they contribute differently to each recorded image. In practice this is achieved by recording images at different relative placements (“phases”) of the illumination intensity maxima (Figure 3a). A lateral translation of the illumination structure leads to a spatial frequency-dependent change of the complex relative phase of the delta peaks to which each shifted object component is attached, thus affecting the phase of each such component individually but uniformly everywhere in Fourier space. All these components are thus differently modulated and can be disentangled by applying an inverse (unmixing) matrix (Figure 3c). Those components that were disentangled from the recorded raw data, of course, still possess the signature of the imaging process: Their contribution is reduced for higher detection spatial frequencies by the multiplication of the emitted light \tilde{E}_m with the optical transfer function \tilde{h} . After placing them at the correct object frequency positions (Figure 3d) and adjusting their phase, we are left with a different transfer function for each such correctly placed object component. It is interesting to note that the original SIM

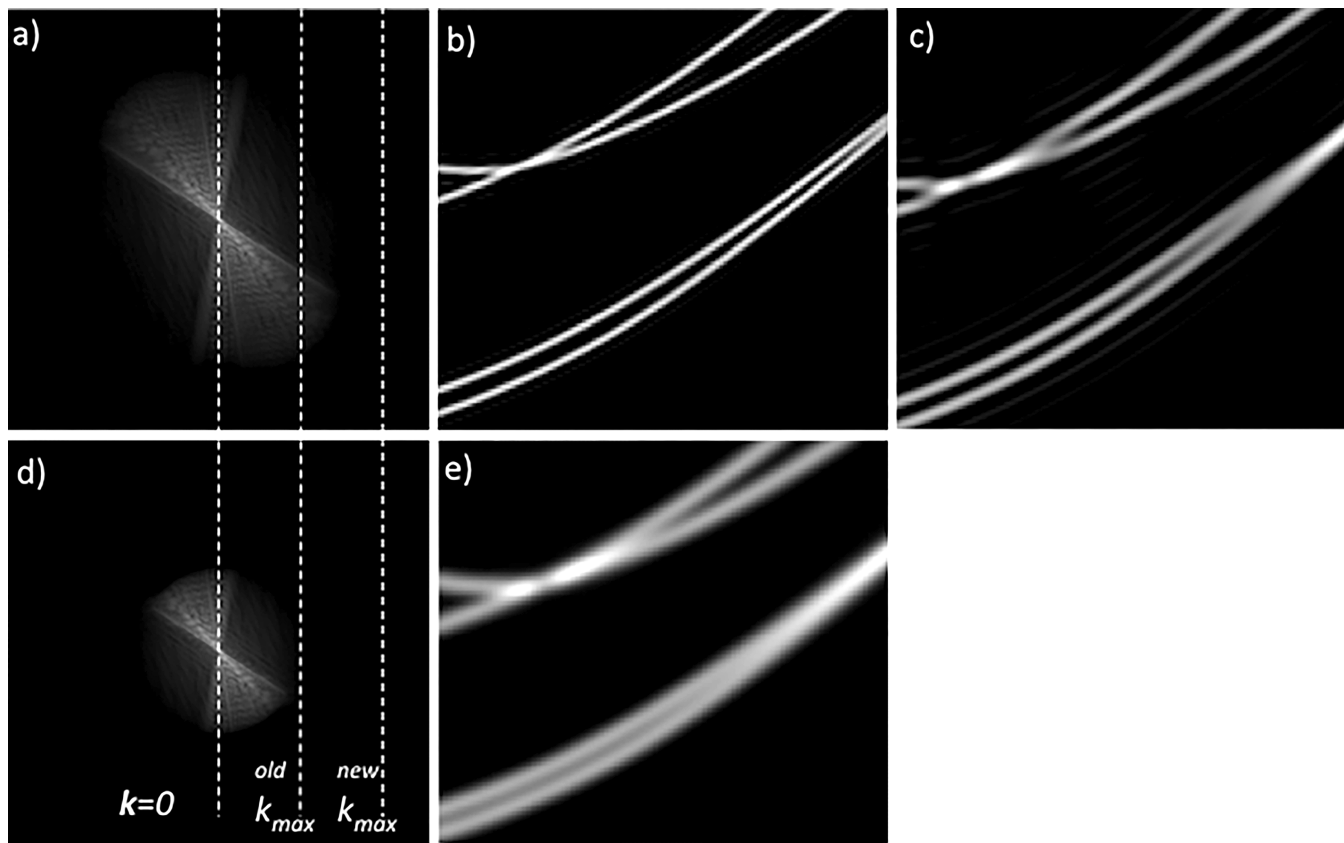


Figure 4. SIM image reconstruction along two dimensions. All separated components are joined (a), Wiener filtered, and transformed back to real space (zoomed region) (b). (c) The same region of the Wiener-filtered wide-field image for comparison. In (d) the Fourier transform of the unfiltered wide-field image (e) is shown.

data in the lateral direction only need to be sampled at the Nyquist limit applicable to wide-field imaging with uniform illumination (see Figure 2h). During the order placement as part of the image reconstruction process, the Fourier space can then be padded with an empty region (Figure 3d) leading to the interpolation of pixel values between the original pixel locations (real space not shown in Figure 3). A typical choice here is to always upsample the data by a factor of 2 in X and Y coordinates by expanding the Fourier space appropriately.

The final reconstruction step is achieved by joining these components at places in Fourier space where they overlap (Figure 3e) by a weighted averaging approach. This is usually performed by calculating a weighted average using the inverse variance (after strength correction) as weights.

This is an essential step where SIM image processing differs from other approaches such as using physical detection pinholes in Nipkow-disk-like systems using masks for excitation and detection. Such systems can be viewed as performing the steps described in SIM reconstruction in hardware, but instead of using a noise-optimized weighted averaging step, they add these separated components in a less optimal way. Similar arguments can also be made about other reconstruction strategies such as the ones used in RESOLFT.²⁷

With only one grating direction, as shown in Figures 2 and 3, only a single-directional resolution gain can be achieved. Therefore, such an illumination phase series has to be acquired typically three times with differently oriented gratings (and polarization). Figure 4 shows the final result of joining three components along three grating orientations (Figure 4a), filtered by a Wiener filter and transformed back to real space

(Figure 4b), which can be compared with the Wiener-filtered wide-field image (Figure 4c). For comparison the wide-field image (Figure 4e) and its Fourier transform (Figure 4d) are also shown.

5.1. The Nitty-Gritty Details of SIM Image Reconstruction

Even though the general process of SIM image reconstruction as described above is straightforward and easy to implement, there are a number of practical complications. To achieve reasonable reconstructions (i.e., minimal reconstruction artifacts), precise knowledge of the illumination structure is needed. This usually cannot be obtained from the instrument directly, even if individual instrument calibration procedures are performed, since it may change from sample to sample or even from one sample position to another. These local variations are typically caused by changes in the local index of refraction or by other system-dependent optical aberrations. Therefore, essential reconstruction parameters such as the precise grating constant and phase for each recorded image need to be determined from the recorded images themselves. It is of great importance to precisely estimate the grating constant and thus the k -vector by which the first order is shifted from the zero order in Fourier space. Trying to detect the modulation directly in the image is not a recommended approach, since at these high frequencies the detection optical transfer function is usually low or has even reached zero as in the case of illumination under total internal reflection conditions. Interestingly, the separation of orders does not require the precise knowledge of the grating constant or the absolute illumination phase of each image but can rely on the approximate

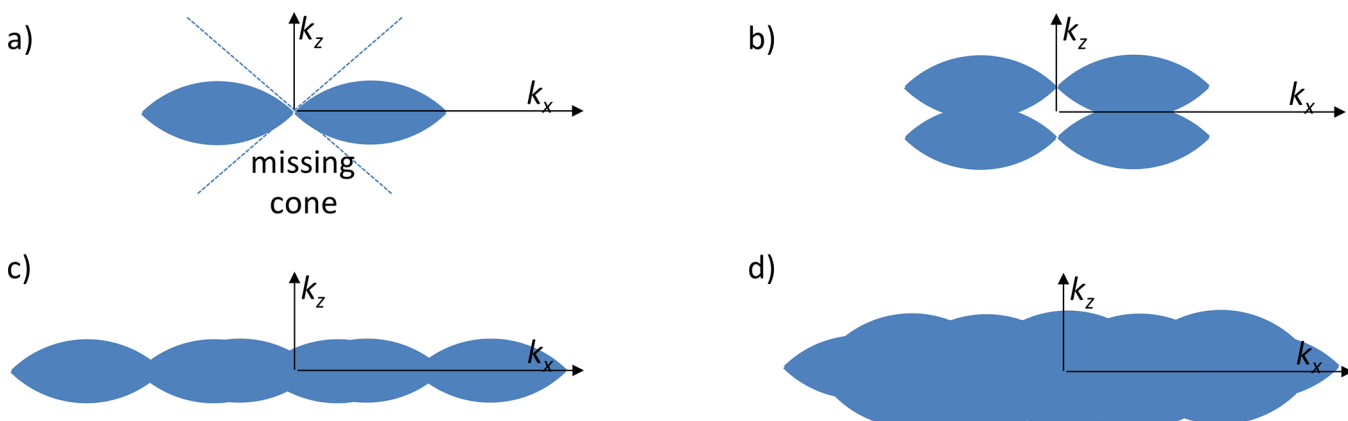


Figure 5. Optical transfer functions (OTFs). Central $k_x - k_z$ cross section of the region of support of the detection OTF under uniform illumination (a). This also applies to the OTF for detection of the zero component and, if the illumination is fully coherent also to the second component. The detection OTF first order of three-beam SIM is shown in (b). Final OTFs of reconstructed two-beam (c) and three-beam SIM (d) imaging (one grating direction only) using a grating vector slightly lower than the finest possible grating. Note that multiple directions fill the gaps along k_z in (d).

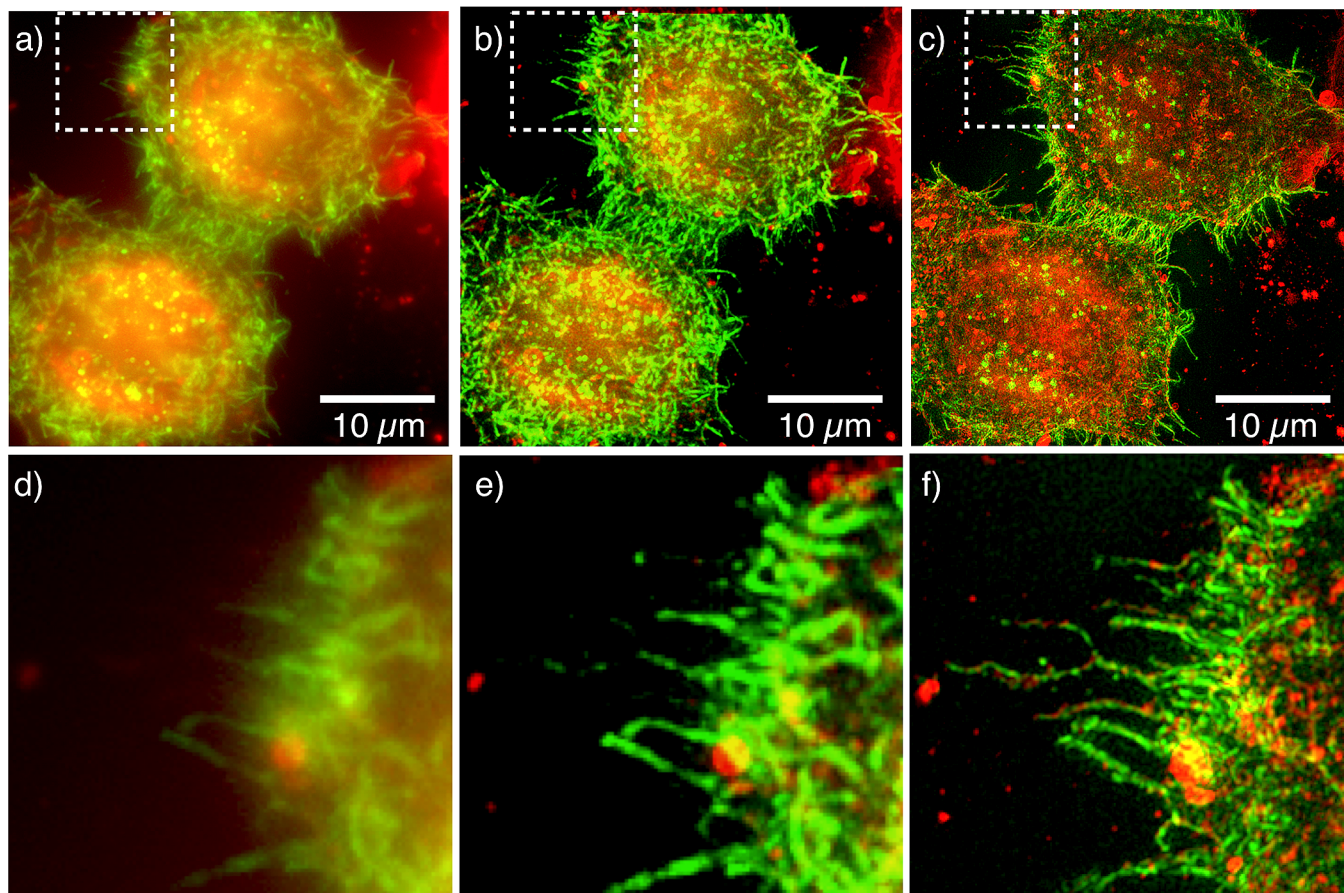


Figure 6. Maximum intensity projection micrographs of osteosarcoma (U2OS) cells shown in wide-field epifluorescence (a), deconvolution of the epifluorescence data (b), and 3D-SIM (c). The green color channel encodes for transmembrane β -dystroglycan-eGFP subunit, while the red color channel highlights the plasma membrane stained with CellMask orange. Magnified views of the boxes highlighted in the upper row are shown in the lower row, (d)–(f).

knowledge of the relative phase between individual images. Luckily, such separated but neighboring orders usually have significant overlap (especially in three-beam SIM) which can be exploited. The standard approach, therefore, is to iteratively maximize the frequency-weighted cross-correlation at zero frequency between the zero and the first separated orders shifted in Fourier space by the k -vector that is iteratively being

optimized. This integral can be efficiently evaluated in real space after the frequency weights have been applied. Notably, an error of more than 1/10th of a pixel in Fourier space can already lead to visible artifacts in the reconstructed image. From the same optimization also the global phase of the separated order can be obtained by evaluating the complex phase of the cross-correlation.⁵²

In many cases the aforementioned separation by unmixing can contain residual orders due to imprecise individual illumination phases or due to patterns being bleached into the sample during data acquisition. This can be accounted for by iteratively minimizing the residual presence of such unwanted orders. However, it is also possible to determine the individual phases from the weighted autocorrelation at the precise grating frequency of each image.⁵¹

As usually limited volumes are acquired along the axial direction, significant problems can be caused by out-of-focus light in the reconstruction. At illumination frequencies below the detection Abbe limit, 2D-SIM can be equipped with optical sectioning capability, albeit usually at the cost of a slightly reduced spatial resolution, by utilizing a method called OTF attenuation. In OTF attenuation it is exploited that, at low detection spatial frequency, where the OTFs have a missing-cone problem, information can be more reliably substituted from other separated orders. Thus, the OTF and the data are artificially reduced at the central passband. It can also be helpful to replace the Wiener filtering step by a positivity constrained iterative deconvolution. Note that, for data sets obtained by three-beam illumination, the missing axial information near zero lateral spatial frequency, provided that the illumination frequency is not too close to the border of the detection passband, can be replaced by information from the shifted first-order band, which provides the ability of single slice reconstructions with rejection of out-of-focus contributions.⁵³

It should also be noted that, in SR-SIM with total internal reflection illumination (TIRF-SIM), a spatial resolution of more than 2 times the Abbe limit can be achieved due to the often substantially higher excitation NA, which is fully exploited through this illumination scheme. The consequences of this will be discussed further in section 9.

5.2. The Complications of 3D-SIM

The image reconstruction steps described above form the basis of SR-SIM image reconstruction. However, the arguments were only based on a flat two-dimensional sample placed in the focal plane of the microscope. In a proper 3D-SIM system a series of SIM images is acquired for each focus position and the sample is stepped through the focus in small vertical steps. Since the illumination structure generated in a three-beam SIM system also generates an axial intensity structure and this structure shifts along Z with respect to the sample coordinate system with changing focus, the axial parts of the illumination structure become imprinted onto the detection point spread function. Only the first order (Figure 5b), not the zero or second order (Figure 5a), will look like it has an in-plane structured illumination but a changed detection PSF consisting of a wide-field detection PSF having been multiplied with an axial sine wave. As a result, the corresponding first order OTF will consist of two copies of a wide-field detection OTF, displaced along the axial direction once above ($+\Delta k_z$) and below ($-\Delta k_z$) the lateral anchoring point (Figure 5b). A direct consequence of this expanded k_z range of the optical transfer function is that the z-sampling in the raw data, i.e., the distance between consecutive slices, has to be twice as fine as required for uniformly illuminated wide-field data or two-beam SIM. This necessitates for the reconstruction process that an individual OTF is needed for each lateral illumination order. In practice it is often difficult to keep the illumination phase in perfect agreement with the slice of best focus. Such a z-shift of the woodpile intensity structure generated in the sample can cause

significant reconstruction artifacts. Therefore, this effect has to be accounted for by an accordingly phase-modified OTF for the first component in the three-beam (five intensity components per direction) setup. This can also be obtained by extracting order separated PSFs/OTFs using a bead sample imaged under the same structured illumination and sample embedding conditions.³³ As an example illustrating the usefulness of 3D-SIM for biological applications, Figure 6 shows a comparison of human osteosarcoma cells (U2OS) stained for dystroglycans (green) and the plasma membrane (red) imaged by wide-field epifluorescence microscopy (Figure 6a, and magnified region of interest, Figure 6d), deconvolution of the epifluorescence image (Figure 6b,e), and 3D-SIM (Figure 6c,f) as maximum intensity projections.

While the continued development of super-resolution microscopy based on single molecule localization has benefited from a community that continuously shared open-access, ready-to-use software packages, SR-SIM image reconstruction algorithms used to be a “black box” for the general user. Fortunately, this situation has changed in recent years and an increasing number of open-source and open-access software packages for SR-SIM image reconstruction have been developed and published. OpenSIM⁵⁴ and Simtoolbox⁵⁵ provide Matlab-based image reconstruction, enabling users and developers to read through the code in a general-use programming language providing high-level mathematics. FairSIM,⁵⁶ on the other hand, provides a platform-independent modular and open-source plugin for ImageJ,⁵⁷ with an easy-to-use user interface implementing most of the automated parameter estimation steps mentioned above. It should be noted that all these image reconstruction packages are currently restricted to the reconstruction of 2D-SIM data (three-beam SIM data can be reconstructed as single slices, but with diffraction limited spatial resolution along the vertical direction). This limitation is due to the complications of 3D-SIM image reconstruction mentioned above, which depend significantly on the optical system and often require the use of system-specific experimental OTFs in order to yield meaningful 3D image reconstructions. This issue is, however, currently also being addressed and will likely be implemented in future versions of these and other software packages. SIMcheck,⁵⁸ on the other hand, is also an open-source ImageJ plugin, but follows a different philosophy. Rather than providing image reconstruction capabilities, it provides a number of useful quality control tools for the analysis of SIM image data, which, e.g., allow users to determine optimum parameters for successful image reconstruction. In addition, SIMcheck also provides calibration and conversion tools that help users of commercial SR-SIM instruments deal with common issues.

5.3. BlindSIM Image Reconstruction

If the illumination structure parameters have been determined, the illumination structure can be assumed to be precisely known. This in turn allows for a different way of reconstructing SIM data based on the principle of inverse maximum likelihood (ML) based algorithms. Such algorithms are the basis for ML deconvolution which can be easily modified to include a known illumination structure. An advantage is that these algorithms can work with a fixed set of parameters, obviating the need to choose a different Wiener filter parameter for each reconstruction, and achieve very high quality results. However, they are also orders of magnitude slower than the process of Wiener filtering.

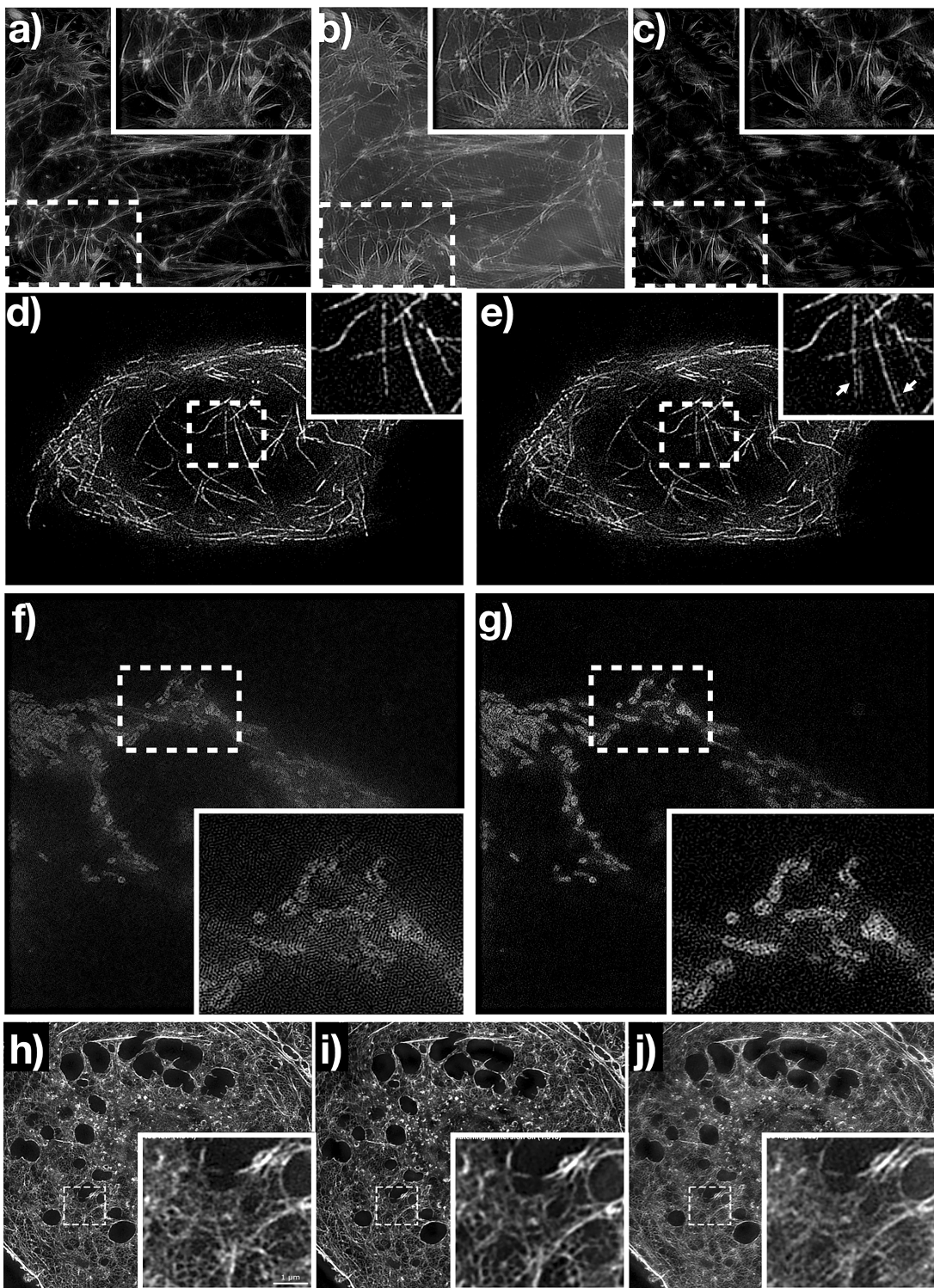


Figure 7. Demonstration of SR-SIM image reconstruction artifacts. Images of the actin cytoskeleton in U2OS cells reconstructed using (a) automated parameter estimation combined with OTF attenuation, (b) the same image without OTF attenuation, and (c) angle setting of one pattern direction deliberately set off by 5° . Images of the tubulin network in a U2OS cell with (d) correct parameters and (e) k_0 estimated wrong by 5%. Noisy data sets of mitochondria in U2OS cells stained by Mitotracker Red reconstructed with a Wiener parameter of (f) 0.001 and (g) 0.009, respectively. The effect of spherical aberrations is demonstrated by imaging the actin cytoskeleton stained with phalloidin conjugated to Alexa Fluor 488 with immersion oils with refractive indexes of (h) 1.514, (i) 1.518, and (j) 1.522.

Particularly interesting are methods which do not require precise knowledge of the illumination pattern but estimate it along with the iterative reconstruction. Although such algorithms are even slower than ordinary SIM deconvolution, their beauty is that they are able to also reconstruct aberrated

illumination patterns. In extreme cases even reconstructions with random (speckle) illumination are possible,⁵⁹ albeit typically requiring hundreds of raw images for a single reconstruction. By reconstructing a three-dimensional volume from just single-plane data and discarding all other planes,

efficient removal of out-of-focus signal is also possible.⁶⁰ Even though this approach is a current trend in focusing on improving SR-SIM image reconstruction, it should be kept in mind that speckle illumination patterns contain far less energy at high spatial frequency than standard two- or three-beam illumination patterns.

5.4. Avoiding SR-SIM Image Reconstruction Artifacts

As already discussed earlier, as a wide-field imaging method, SR-SIM is particularly sensitive to a number of issues that can result in sometimes severe image reconstruction artifacts. Small deviations of the reconstruction parameters from the correct parameters often lead to ghosting or fringing artifacts that are noticeable in the reconstructed images, requiring iterative adjustments to the parameters and continued image reconstruction in order to minimize such artifacts. As examples, the first row of Figure 7 shows a selection of images containing artifacts based on a real 3D data set of U2OS cells where the actin cytoskeleton was stained with an antibody conjugated to an organic fluorophore (Alexa Fluor 647). Figure 7a shows an image where all parameters were chosen by automated parameter estimation algorithms and OTF attenuation was used to reject fluorescence from outside the focal plane. The inset is indicated by the dashed frame and shown magnified in the upper right corner of each image. Figure 7b shows the same image, but without OTF attenuation. The additional fluorescence contributions excited by the three-dimensional excitation pattern lead to considerable fringing in the reconstructed image. Figure 7c shows an image where OTF attenuation was used, but the angle of one pattern direction was deliberately set off by 5°. As can be seen from this image, this leads to long-range intensity variations (coarse dark fringes) in the pattern direction with the incorrect angle that spreads across the entire image. Failure of the algorithm to correctly estimate all parameters can also lead to some of the filaments in the image appearing to have been split into two, which can easily be mistaken as a feature of the sample, if one does not pay attention to such effects. Figure 7d,e demonstrates this more clearly with images of a U2OS cell where the tubulin cytoskeleton was immunostained with Alexa Fluor 647. In Figure 7d the correct parameter set was used for the reconstruction, whereas in Figure 7e k_0 was deliberately estimated wrong by 5% in both angle and length, resulting in prominent split-fiber artifacts.

Data sets containing considerable noise are also often very difficult to reconstruct. Currently, noise contributions are typically handled by setting the Wiener parameter in the Wiener filter to higher values. We demonstrate this in the example of a 3D data set of mitochondria in U2OS cells stained with the cell permeable fluorophore Mitotracker Red. Figure 7f shows an image reconstructed with a low Wiener parameter of $\omega = 0.01$, resulting in poor contrast and considerable fringing in the reconstructed image. In Figure 7g the Wiener parameter was set to $\omega = 0.09$, resulting in significantly improved contrast and reduced noise-related fringing artifacts. Unfortunately, at the present time, this effect has to be minimized “by hand” and depends on the individual user performing the image reconstruction. The development and implementation of better noise models into future versions of the image reconstruction routines should permit more quantitative comparisons and reduction of such noise-induced effects.

Another significant source of image artifacts are spherical aberrations which high NA microscope objective lenses are

particularly prone to. Unfortunately, the degree to which spherical aberrations distort wide-field images depends on a range of parameters, such as the cover glass thickness, the index of refraction of the medium in which the sample is embedded, as well as the index of refraction of the immersion oil, and even the sample temperature. This effect is demonstrated in Figure 7h–j for the example of primary rat endothelial cells where the actin cytoskeleton was stained with phalloidin conjugated to Alexa Fluor 488. Figure 7i shows a result where the immersion oil was chosen to minimize spherical aberrations (refractive index 1.518). In Figure 7h the index of refraction of the immersion oil was chosen too low by 0.004, whereas in Figure 7j it was too high by 0.004. As can be seen from the images, this greatly affects image contrast and sharpness. Spherical aberrations could be improved by implementing adaptive optics into the imaging path of an SR-SIM microscope, but this is still a fairly expensive solution compared to choosing the proper immersion oil.

6. ALTERNATIVE APPROACHES TO SR-SIM

From a fundamental point of view, confocal microscopy can also be considered as an implementation of structured illumination, because the illumination light is structured to produce a diffraction limited spot, which is then scanned across an otherwise homogeneously fluorescent sample. Here, in order to extract out-of-focus contributions from all directions, a pinhole placed in a conjugate image plane in front of the detector, when narrowed down to a diameter less than the diameter of the Airy disk of the magnified focus spot, can enable one to resolve lateral structures down to $\sqrt{2}$ of the diffraction limit,⁶¹ also improving the passband by a factor of 2. A problem of this approach is, however, that the amount of light reaching the detector is also significantly reduced. A much better approach is to “reassign” the origin of the photons on the detector—a concept that was initially realized in a theoretical derivation by Colin Sheppard.⁶¹ This concept does not sacrifice out-of-focus photons, while still enabling a resolution gain of up to 1.53 compared to the conventional diffraction limit. The experimental implementation was then demonstrated in 2010 by Müller and Enderlein, who imaged the fluorescence obtained from each confocal spot onto an electron-multiplying CCD camera and reconstructed the image mathematically from the information collected from all the images obtained for each position of a confocal scan.⁶² This concept has also found its commercial implementation in the Zeiss 880 “Airyscan” confocal laser scanning microscope. An extension of this concept, utilizing a deconvolution-based image reconstruction approach, was then demonstrated by York et al.⁶³ Here, the authors parallelized the previous implementations by creating hundreds of confocal illumination spots that are imaged onto a CCD camera. Cropping the spots by virtual pinholing and decreasing the spot size while maintaining spot separation, this enabled the authors to achieve a performance similar to that of Müller and Enderlein, but requiring the acquisition of only about 200 images in total. This was followed by similar implementations using spinning disk confocal microscopes.^{64,65} More recently, this approach was also demonstrated with two-photon fluorescence excitation, enabling multifocal multi-photon fluorescence microscopy with approximately 1.5 times higher spatial resolution even in thicker tissue slices.⁶⁶ It was soon realized, however, that the computational image reconstruction is not really necessary in this case and an all-optical image formation can be utilized. Different implementa-

tions of this concept have been realized, but they all typically utilize a similar concept, where images of confocal fluorescence spots are optically compressed (reduced in width by a factor of 2), while maintaining their distance with respect to each other, before imaging them onto a CCD camera. Alternatively, if the size of the foci remains unaltered, the same effect can be achieved by increasing the distance between the spots by a factor of 2 before imaging them onto the camera.^{67–69} In an impressive extension of this concept, York et al., again, turned this approach into a multifocal mechanism with separate optical compression path, enabling them to image, e.g., the dynamics of the endoplasmic reticulum in living human lung fibroblasts at 100 frames s⁻¹, and even vascular flow in zebrafish embryos.⁷⁰ The concept of all-optical photon reassignment microscopy also readily applies to two-photon fluorescence excitation, enabling high lateral resolution (150 nm), high speed (1 frame s⁻¹) imaging of microtubules in the eye of a living zebrafish embryo at depths exceeding 100 μm.⁷¹ Comparing these approaches to standard SIM using sinusoidal illumination patterns, it should be noted that the focused laser beam illumination is generating significantly less high spatial frequency, which in turn leads to a lower signal-to-noise performance at the highest resolution. Recent approaches utilizing Bessel-beam illumination or conical diffraction patterns are able to improve upon this.

Unfortunately, a large number of different terms have been coined by authors with regard to naming this photon reassignment process. They range from image scanning microscopy (ISM), photon reassignment microscopy, rescan confocal microscopy, to (rather confusingly) specializations of SIM, such as “instant SIM” or “multifocal SIM”. Please note that in the context of this review article we strictly refer to SR-SIM whenever high-contrast sinusoidal interference patterns are used, with the advantage being that only SR-SIM can achieve efficient true resolution doubling (or more, in the case of TIRF-SIM) compared to these other processes.

7. COMBINING SR-SIM WITH OTHER SUPER-RESOLUTION MODALITIES

Another interesting concept stems from the fact that SR-SIM as a wide-field imaging method is readily compatible with other super-resolution optical microscopy methods, such as single molecule localization microscopy and stimulated emission depletion. As we will see in section 8, both these concepts have been exploited in combination with SR-SIM to further extend the spatial resolution of SR-SIM. In another implementation, SR-SIM can also be readily coupled with photoactivated localization microscopy (PALM) or stochastic optical reconstruction microscopy (STORM) in order to complement SR-SIM with the even higher spatial resolution provided by these methods. This enabled Rossberger et al. to correlate and compare images acquired with both methods in order to identify imaging artifacts and to obtain higher structural details in HEK293 cells.⁷² Mönkemöller et al., on the other hand, used a similar approach but took advantage of the higher speed, but lower resolution afforded by SR-SIM to survey a sample of liver sinusoidal endothelial cells, and then image sections, where sieve plates with a large number of fenestrae were present, by STORM, and correlate these image data to allow them to determine that individual fenestra are stabilized by rings of actin fibers, while sieve plates are segregated by thick bundles of tubulin and actin.⁷³ We expect such correlative studies to further increase in frequency in the

years ahead, once more researchers begin to take advantage of the unique properties of each method, possibly even extending to live cell studies, where, e.g., cellular physiology is initially followed at high resolution and high speed at 37 °C, followed by reversible cryo-arrest for high-resolution structural imaging by single molecule localization microscopy.⁷⁴

8. INCREASING THE RESOLUTION BEYOND A FACTOR OF 2: NONLINEAR SR-SIM

Linear SIM yields roughly a factor of 2 in resolution improvement, when neglecting the small wavelength difference and assuming that the illumination is being directed through the same objective lens also used for detection. As mentioned previously, the way to break free from these constraints is by exploiting nonlinear effects, most easily implemented by invoking a nonlinear or multilinear sample response. If a sample responds nonlinearly to the illumination pattern, then the emitted signal will contain this nonlinear response in the form of higher harmonics seemingly belonging to the Fourier spectrum of the illumination structure to which the sample information is attached. Although this information will be filtered by the transfer function of the microscope, high-frequency information will, again, be mixed to lower frequencies and can be restored computationally. Here, the “emittability” takes over the role of the illumination intensity in linear SIM. The emissibility is a nonlinearly deformed version of the illumination intensity or a combination of several structured illumination patterns acting on photoswitchable fluorophores.²⁴ The linear far-field imaging path of the microscope can then image the encoded information by transferring only low frequency information and the reconstruction algorithm reconstructs the high-resolution image in just the same way as previously described. Of course, since in nonlinear SR-SIM even more higher order components are present, more raw images, i.e., more phases and more directions, need to be acquired in order to facilitate successful isotropic image reconstruction. As the algorithms assume that the sample is homogeneously labeled and emits constant fluorescence during the acquisition of all the images required for one reconstruction, it is important to acquire all required images at a speed that is significantly faster than any cellular processes in order to avoid motion artifacts.

The simplest form of a nonlinear sample response that could be utilized for this purpose is debatably the induction of direct singlet state saturation by a very high illumination intensity. This effect is well-known by most scientists who have used a confocal microscope. All fluorophores can at most emit approximately one photon per fluorescent lifetime regardless of how strong an illumination intensity one ultimately uses. The singlet state saturation conditions are usually best achieved for wide-field illumination by using a laser producing intense nanosecond pulses.⁷⁵ A disadvantage is that excitation pathways from the singlet or triplet state can easily lead to rapid sample degradation or even destruction and the momentary thermal load during the pulse can also lead to too much heat generation. Another disadvantage of this direct-saturation scheme is that under strong saturation most fluorophores are uniformly fluorescing and only a few are not. The latter yield the essential high-resolution information, whereas the many fluorescing molecules just contribute to the overall background. This can be called a “negative contrast scheme”. The disadvantage here is a worse signal-to-noise performance compared to positive contrast schemes such as STED and

the fact that fluorescing molecules are more prone to photobleaching than nonfluorescing ones, because photobleaching is an excited state photochemical reaction often involving multiple photons.

A good alternative is the use of photoswitchable fluorescent dyes.^{50,24,49,50,75} Here, the nonlinear dependence is generated by the saturation of the transition from the on state to the off state of the fluorophores. This alleviates the two disadvantages mentioned above: Since activation, depletion, and readout can individually be controlled and performed with individual spatial patterns, positive contrast can be generated. Even if strong saturation is avoided to maintain sample viability, a multilinear combination²⁴ of activation, depletion, and readout can lead to ~60 nm spatial resolution for extended imaging times, enabling one to record seemingly unperturbed videos of living cells.⁵⁰

A significant complication of photoswitching-based nonlinearities is that a single molecule is digitally in either the off state or on state. This leads to super-Poissonian noise perturbing the current SIM reconstruction strategies. If we imagine imaging only a single molecule at a position where it has a 50% chance of remaining in the on state during readout, in this simplified picture this would lead either way (it remains on or off) to an entirely wrong reconstruction result, as the algorithm assumes 50% brightness. Detecting thousands of photons from a single molecule is of no use here, and in principle a single detected photon per switching cycle would yield almost the same amount of information. As a consequence, it pays off to trade the brightness of the individual molecules for their ability to switch a large number of cycles without destruction. Indeed, this problem is what has driven recent developments in synthesizing new fluorescent dyes which can tolerate a large number of switching cycles.⁷⁶

9. APPLICATIONS OF SR-SIM TO CELL BIOLOGY

To date, commercial implementations of SR-SIM are available from three major microscope manufacturers. These systems are all capable of 3D imaging at up to four color channels and are widely used in imaging facilities, mostly as replacements or extensions of other fluorescence microscopes, such as laser scanning confocal microscopes or fluorescence deconvolution microscopes. The speed with which the illumination pattern is created and moved through the sample, as well as the image acquisition time in some of these commercial units, is currently not optimized for live cell imaging, which has applications demonstrated by these machines limited to mostly structural studies of cell biology in fixed cells. Only a few of these commercial units are currently targeted toward live cell imaging applications. Thus, to date, the majority of SR-SIM publications mostly report on the structural biology of fixed samples, while the observation of living cells is slowly emerging in the form of time-lapse studies. At the same time, a large number of research groups around the world are actively developing and utilizing custom-built implementations of SR-SIM and they are continuing to push the envelope in terms of imaging speed, spatial resolution, and sensitivity. In this section we briefly revisit some of the most remarkable achievements in cell biology utilizing SR-SIM.

Schermelleh et al. presented the first major case for the use of 3D-SIM in the structural analysis of the chromatin distribution in nuclei of mammalian cells. They utilized 3D-SIM in up to three different color channels to simultaneously visualize chromatin in fixed mouse C2C12 myoblast cells, along with the nuclear lamina and the nuclear pore complex.⁷⁹ The

extensive 3D imaging capability of their system allowed them in particular to resolve individual nuclear pore complexes which colocalized with channels in the nuclear lamina. They were also able to distinguish different pore complex proteins on the inner and outer nuclear membrane. Voids in the DNA structure leading up to nuclear pore complexes suggested that DNA is excluded from these pores that connect the cytoplasm with the nucleus. This early work made an impressive case for the usefulness of three-dimensional resolution doubling in wide-field fluorescence microscopy, the simultaneous imaging of multiple color channels, and the use of conventional fluorophores for labeling cellular structures of interest. Wang et al. then used 3D-SIM in a remarkable validation of this method in comparison to electron microscopy to image and analyze the synaptonemal complex in meiotic chromosomes of maize, where the lateral elements of these structures are just below the limit that can be resolved by conventional optical microscopy.⁷⁸ By using DNA intercalating fluorophores and fluorescently labeled antibodies against the cohesin REC8 α -kleisin homologue, they found that the distribution of this protein is discontinuous along lateral elements, that coiling of the DNA occurs after the formation of synaptonemal complexes, and that these complexes are coiled as left-handed double helical structures. By analyzing these structures throughout meiosis, they were also able to reveal the transient nature of these interlocks during different stages of meiosis. This work on chromatin structure was rapidly followed by additional 3D-SIM studies that analyzed the structure of human centrosomes at different stages of the cell cycle, i.e., mitosis or interphase.⁷⁹ The high specificity of fluorescently stained antibodies and the extended three-dimensional imaging depth of SR-SIM make it an invaluable tool in analyzing, e.g., the colocalization of structural proteins in all dimensions. By complementing such high resolution structural studies with live cell imaging, Chagin et al. recently demonstrated the visualization of replication foci down to single replicons.⁸⁰ Even biomedical applications of SR-SIM are now beginning to emerge. In an early example, Brown et al. used 3D-SIM to determine that cortical actin remodels near immune synapses of natural killer cells.⁸¹ This remodeling of the tight actin mesh is believed to create the space needed for natural killer cells to secrete lytic granules to target cells in order to kill virus-infected or transformed cells. Cogger et al. were the first to image the structure and distribution of fenestrae, nanosized pores in liver sinusoidal endothelial cells by fluorescence microscopy, which, until then, could only be studied by electron microscopy, which caused some biologists to believe that these structures might be artifacts due to the harsh sample preparation required for electron microscopy.⁸²

Similarly, Regev-Rudzki complemented a vast amount of biochemical analysis techniques with SR-SIM to reveal that red blood cells infected with *Plasmodium falciparum*, the parasite causing malaria, utilize exosome-like vesicles to enable communication between parasites.⁸³ And, in related work, by using viable *P. falciparum* merozoites, Riglar et al. were able to investigate how the parasite exports proteins and remodels the structure of erythrocytes in order to ensure the survival of the parasite inside infected cells.⁸⁴

Indeed, microbiology is another area that has rapidly adopted the new possibilities enabled by SR-SIM. A number of studies have focused on the structure and distribution of FtsZ, a bacterial homologue of tubulin in eukaryotic cells, which assembles into a so-called Z ring leading up to bacterial cell

division. Strauss et al. used 3D-SIM to show that Z rings in *Bacillus subtilis* and *Staphylococcus aureus* are patchy and discontinuous rather than forming a continuous structure.⁸⁵ Time-lapse imaging enabled them to reveal that FtsZ localization with the Z ring is dynamic and remains heterogeneous throughout the cell division process. Rowlett and Margolin then showed that this same patchy distribution of FtsZ is also found in *Escherichia coli*.⁸⁶ Also, in *Escherichia coli*, Lesterlin et al. used 3D-SIM to follow the progression of the repair of DNA double-strand breaks in living bacteria cells.⁸⁷ They were able to determine the sequence and stoichiometry at which different bacterial enzymes have to congregate at the site of DNA double-strand breaks in order to recognize and repair the local damage. In particular, they found that the repair enzyme RecA forms bundles to facilitate the search for damage sites. A recent study by Bisson-Filho and co-workers made extensive use of 3D-SIM to shed new light on the dynamics and location of enzymes involved in bacterial cell division.⁸⁸ By using pulse-labeling of dividing bacteria with fluorescent amino acids, they found that the peptidoglycan septum is progressively synthesized from the cell surface inward and that synthesis occurs at discrete sites that circle around the division plane. This enzymatic activity was found to be controlled by dynamic treadmilling of FtsZ filaments. This work is a particularly nice demonstration of how new biological insights can be gained by the full three-dimensional resolution doubling achieved by SR-SIM, which enabled the visualization of these discrete peptidoglycan synthesis sites in 3D.

SR-SIM has also begun to be utilized in the analysis of viral structure. In a recent example, Horsington et al. used 3D-SIM to image single vaccinia virus particles to follow virus maturation and morphogenesis in a fluorescent clone of this member of the poxvirus family.⁸⁹ Notably, again, the three-dimensional nature of 3D-SIM allowed them to resolve the viral envelope protein B5 as a spherical structure surrounding the virus core, which provides a means of judging the degree of maturation of virus particles. Particularly helpful in these recent biological studies is also the aspect that SR-SIM is compatible with most fluorophores and does not require the use of specific photoactivatable or otherwise optimized fluorophores. This significantly lowers the threshold for successful biological applications.

A surprising number of papers have been published with SR-SIM applied to plant cell structure. In particular, the structure of plasmodesmata, microscopic channels that enable transport and communication between plant cells, and their involvement in the trafficking of plant viruses have been the topic of recent studies. Fitzgibbon et al. used 3D-SIM to resolve components of plasmodesmata in leaf parenchyma cells of tobacco.⁹⁰ This was followed by Tilsner et al., who showed how movement proteins of the potato virus X modify plasmodesmata to cross the plant cell wall.⁹¹ Live cell imaging of viral RNA and virus-related proteins allowed them to visualize how movement proteins compartmentalize replication complexes at plasmodesmata to localize RNA synthesis and promote the directional trafficking of virus between cells. Linnik et al. then used 3D-SIM to unravel the structure of viral replication complexes of potato virus X.⁹² More recently, Wanner et al. used SR-SIM to analyze the structure of plant chromatin, in particular the association and distribution of centromere-associated proteins with plant chromosomes.⁹³ Also, Schubert and Weisshart used SR-SIM and single molecule localization microscopy to determine and quantify the distribution of RNA polymerase

II, the enzyme responsible for the transcription of protein-coding genes, in nuclei of *Arabidopsis thaliana*. Interestingly, they found that this enzyme indeed forms aggregates within the chromatin, albeit in structures smaller than the transcription factories found in mammalian cells.⁹⁴

As of this writing, most live cell imaging data acquired with imaging times of a few seconds or even below 1 s per super-resolved image are still generated on custom-built SR-SIM systems. Key for live cell imaging is the speed with which the illumination pattern can be generated and swept across the sample, which, to date, has been realized by utilizing electrooptic devices, such as spatial light modulators. The initial implementations were achieved with a single excitation wavelength. Kner et al. demonstrated live cell imaging of tubulin and kinesin dynamics in *Drosophila melanogaster* S2 cells at 11 frames s⁻¹ using a TIRF implementation of SR-SIM.³² Roughly at the same time, Hirvonen et al. demonstrated 3D-SIM time-lapse imaging of mitochondria movement in a living COS-7 cell.²⁰ Shao et al. followed this up with fast 3D-SIM imaging of mitochondria in HeLa cells and microtubules in *Drosophila* S2 cells at speeds of 5 s per volume and up to 50 time points.⁹⁵ Multicolor imaging of mitochondria in HeLa cells, clathrin-coated vesicles and the actin cytoskeleton in HeLa cells, as well as filopodia and lamellipodia in living neurons at rates of 8.5 s per volume in two colors was later demonstrated by Fiolka et al.⁹⁶ The continued development of fast 3D SR-SIM imaging studies at multiple colors clearly depends on even faster implementations of SR-SIM pattern generation as well as synchronized camera readout, which has been demonstrated (for now in 2D) at rates as fast as 20 super-resolved frames s⁻¹,⁹⁷ and more recently even 79 super-resolved frames s⁻¹ in reduced fields of view.⁹⁸

In an effort to adapt nonlinear SR-SIM to live cell imaging, Li and colleagues recently demonstrated NL-SIM in the investigation of rapid, membrane-near uptake processes, such as endocytosis and exocytosis either through clathrin-coated pits or through caveolae.⁵⁰ They also imaged how the actin cytoskeleton is involved and remodeled during these processes. The impressive speed and spatial resolution below 100 nm in this work was accomplished by utilizing TIRF-SIM through a microscope objective lens with an exceedingly high numerical aperture of 1.7, which permitted the visualization of actin fibers at 84 nm resolution and high speed. To obtain even higher spatial resolution, this concept (albeit implemented with an NA 1.57 objective lens) was also used in combination with an intricate switching scheme of a photoactivatable fluorescent protein. In this implementation of NL-SIM, the photoactivatable fluorophore was kept in the off state for the majority of the time. Exposure of the sample to a sinusoidal activation pattern with a wavelength of 405 nm was then immediately followed by a sinusoidal excitation pattern at 488 nm. The two sinusoidal standing wave patterns had to overlap precisely in TIRF mode across the entire field of view. The achromatic overlap between the activation and excitation pattern permitted low activation and excitation intensities that prolonged the lifetime of the sample and kept phototoxicity to a minimum. This intricate combination of activation and excitation pattern as well as the use of the high NA objective lens allowed Li et al. to acquire the bare minimum of raw images frames (25 images (5 phase × 5 angles)) to successfully reconstruct images of living cells with close to 60 nm spatial resolution. Unfortunately, the minimalism with regard to the number of raw images, as well as the low signal-

to-noise ratio accompanying this imaging procedure, comes at the expense of more noticeable image reconstruction artifacts.^{99,100}

In an impressive brute-force approach utilizing several super-resolving optical microscopy schemes, Nixon-Abell et al. utilized primarily SR-SIM and related methods (TIRF-SIM at an angle just below the critical angle in order to achieve an extended vertical illumination depth, as well as 3D-SIM) to determine the structure and dynamics of the endoplasmic reticulum (ER) in the peripheral parts of U2OS and COS-7 cells.¹⁰¹ They used this, in conjunction with other techniques that provide higher structural detail in fixed cells, as well as correlation with focused ion beam and scanning electron microscopy, to observe the rapid assembly and disassembly of sheet-like ER structures into tubules that exhibited substantial motion similar to tubular oscillations on time scales as short as 0.25 s.

10. CONCLUSIONS AND PERSPECTIVE

SR-SIM is a fast growing field, from both a user's and a developer's perspective, offering optical super-resolution also for living specimen. SR-SIM nicely bridges the gap between the highly versatile wide-field fluorescence or laser-scanning confocal microscopes and electron microscopes. It utilizes the high specificity of molecularly specific labeling, either in the form of fluorescent protein fusions or through antibody labeling, the extended 3D imaging capability, and its potential for live cell imaging. As an imaging modality that does not place special requirements on fluorophores and readily works with samples that are stained for confocal fluorescence microscopy, SR-SIM is a super-resolution imaging method that has already made substantial contributions to cell biology and will continue to do so in the near future. It readily extends to live cell imaging as well, although the requirement of having to acquire several images per focal plane, as well as having to move through the sample at smaller step sizes in the axial direction, places constraints on the highest imaging speed that can be achieved in SR-SIM live cell imaging. The most severe limitations in this regard are placed on 3D imaging by SR-SIM, because 3D image reconstruction typically requires the use of images taken at several different focal planes to yield high-quality image reconstructions. Here, sample motion, i.e., a cell's migration along a surface, will interfere with the reconstruction process, leading to motion artifacts. This is an area where a number of recent and new developments can have significant impact in the future, e.g., through the use of diffractive optical elements to simultaneously acquire multiple images in different focal planes¹⁰² or by developing software and hardware methods that can compensate for sample movement. Also, adaptive optics, which has already been utilized in custom implementations of SR-SIM, will likely see novel applications in this area beyond the correction of pure imaging artifacts such as spherical aberrations. In the same context we also expect to see continued improvements being made in the use of novel image reconstruction methods that can compensate for noise in images, such as the application of denoising filters or the implementation of specific noise models as part of the reconstruction process, or in the more simplified use of blindSIM image reconstruction approaches that do not require precise knowledge of parameters related to the illumination pattern.

Another, currently fairly significant limitation of SR-SIM is its imaging depth, in particular when used for imaging tissue. Here,

the quality of coherent beams that interfere at defined locations with greater distance from the substrate is often compromised by scattering and back-reflection of the beams within the dense tissue. To some extent this can be compensated for by adaptive optics, but it will likely require other approaches as well. We also expect to see further advances being made in the combinations of light-sheet and SIM technology as well as high-resolution lattice light-sheet implementations. Another promising approach is the combination of limited "region-of-interest" illumination for deep tissue SIM with or without two-photon excitation.¹⁰³

Currently, in the majority of implementations, SR-SIM is limited to the linear case, i.e., to doubled optical resolution in all directions. TIRF-SIM utilizing high NA microscope objective lenses has extended beyond a factor of 2 and demonstrated approximately 84 nm resolution in the lateral direction. Nonlinear implementations can overcome this barrier, but the use of photoswitchable fluorophores makes sample preparations for applications more cumbersome. At this time, the number of research groups working in this direction is still fairly small. This development also crosses the barrier to other super-resolution modalities, such as stimulated emission depletion at low depletion laser power, or RESOLFT. These developments will benefit from the continued progress being made in the creation and the use of novel fluorescent proteins. In particular, functional fluorescent proteins, such as the recently demonstrated kinase activity sensors,¹⁰⁴ will likely also be a driver for new (faster and more highly resolving) imaging instrumentation. We, thus, believe that this area will progress and we will see more applications, at least for the cases of 2D-SIM and TIRF-SIM, but it might become more difficult in the future to clearly label any such developments as progress resulting from just one particular super-resolution modality. Even nonlinear 3D-SIM has been demonstrated in combination with lattice light-sheet illumination and should see continued improvements in simplifying the instrumentation required to obtain such images. As a full-field, camera-based imaging technology, SR-SIM will benefit from future developments in this fast-growing field driven by consumer electronics, so that increased performance at lower price points can also be expected. These technological developments will likely be the main driver, leading to more robust and inexpensive implementations of SR-SIM in the near future.

ASSOCIATED CONTENT

Special Issue Paper

This paper is an additional review for *Chem. Rev.* 2017, 117 (11), "Super-Resolution and Single-Molecule Imaging".

AUTHOR INFORMATION

Corresponding Authors

*E-mail: heintzmann@gmail.com.

*E-mail: thomas.huser@physik.uni-bielefeld.de.

ORCID

Thomas Huser: 0000-0003-2348-7416

Notes

The authors declare no competing financial interest.

Biographies

Rainer Heintzmann studied physics (major) and computer science (minor) at the University of Osnabrück, Germany, where he received

his Diploma in 1996 working on X-ray scattering at holographic structures written by visible light. He obtained his Dr. rer. nat. degree 1999 in physics under the supervision of Prof. Dr. Dr. Christoph Cremer with work on high-resolution light microscopy using axial tomography and particle localizations. He then continued as a postdoctoral fellow (2000–2002) and junior group head (2002–2004) at the Max-Planck Institute for Biophysical Chemistry in Göttingen, Germany, in the department of Dr. Thomas Jovin. From 2004 to 2015 he headed the “Biological Nanoimaging” group at the Randall Division, King’s College London, U.K., and since 2010 he has been full professor of physical chemistry at the Friedrich Schiller University Jena and head of the Research Department “Microscopy” at the Leibniz-Institute of Photonic Technology, Jena, Germany. His research interests relate to various methods of super-resolution light microscopy (SIM, OPRA, image inversion interferometry) and image processing (deconvolution, inverse modeling). He has published more than 100 peer-reviewed journal articles and book chapters.

Thomas Huser studied physics and computer science at the University of Basel, Switzerland, where he received his Diploma in 1994 while working on near-field optical microscopy. He finished his Ph.D. in 1998 in physics under the supervision of Prof. Dr. Hans-Joachim Güntherodt. In 1998 he joined the Chemistry and Materials Science Division of Lawrence Livermore National Laboratory (LLNL) in Livermore, CA, as a postdoctoral associate and became a staff scientist at LLNL in 2000. In 2005 he became an associate professor in the Department of Internal Medicine at the University of California, Davis, and was Chief Scientist for the NSF Center for Biophotonics Science and Technology at UC Davis. From 2009 to 2011 he was also a visiting professor in the Department of Physics and Technology at the University of Tromsø, Norway. In 2011 he became full professor at UC Davis and then joined the Physics Department at the University of Bielefeld, Germany, while maintaining his position at UC Davis as an adjunct professor. His research interests relate to the application of Raman scattering and single molecule fluorescence detection to biological and medical problems at the single cell level with a particular focus on unraveling processes that occur near the membrane in endothelial cells and in infectious diseases. He has published more than 140 peer-reviewed journal articles.

ACKNOWLEDGMENTS

R.H. acknowledges support by the German Research Foundation (DFG) (TP B5, SFB-TRR 166 “receptor light”, TP C04, SFB 1278 and the project HE 3492/7-1). T.H. acknowledges Grant INST 215/435-1 FUGG from the DFG, and funding from the European Union’s Horizon 2020 research and innovation program under the Marie Skłodowska-Curie Grant Agreement No. 642157, project “TOLLerant”, as well as Grant Agreement No. 766181, project “DeLIVER”. The authors thank Dr. Wolfgang Hübner (University of Bielefeld) for providing fluorescence micrographs comparing different levels of resolution on U2OS cells, and Dr. Viola Mönkemöller for providing images used in the discussion of SR-SIM imaging artifacts.

REFERENCES

- (1) Heintzmann, R.; Cremer, C. Laterally modulated excitation microscopy: improvement of resolution by using a diffraction grating. *Proc. SPIE* **1998**, *3568*, 185–196.
- (2) Gustafsson, M. G. L. Surpassing the lateral resolution limit by a factor of two using structured illumination microscopy. *J. Microsc.* **2000**, *198*, 82–87.
- (3) Engelhardt, K.; Häusler, G. Acquisition of 3D-data by Focus Sensing. *Appl. Opt.* **1988**, *27* (22), 4684–4689.
- (4) Neil, M. A. A.; Juskaitis, R.; Wilson, T. Method of obtaining optical sectioning by using structured light in a conventional microscope. *Opt. Lett.* **1997**, *22*, 1905–1907.
- (5) Lukosz, W. Optical Systems with Resolving Powers Exceeding Classical Limit. *J. Opt. Soc. Am.* **1966**, *56* (11), 1463–1471.
- (6) Lukosz, W. Optical Systems with Resolving Powers Exceeding Classical Limit II. *J. Opt. Soc. Am.* **1967**, *57* (7), 932–941.
- (7) Bachl, A.; Lukosz, W. Experiments on Superresolution Imaging of a Reduced Object Field. *J. Opt. Soc. Am.* **1967**, *57* (2), 163–169.
- (8) Wicker, K.; Heintzmann, R. Resolving a misconception about structured illumination. *Nat. Photonics* **2014**, *8* (5), 342–344.
- (9) Bailey, B.; Farkas, D. L.; Taylor, D. L.; Lanni, F. Enhancement of Axial Resolution in Fluorescence Microscopy by Standing-Wave Excitation. *Nature* **1993**, *366* (6450), 44–48.
- (10) Gustafsson, M. G. L.; Agard, D. A.; Sedat, J. W. (IM)-M-5: 3D widefield light microscopy with better than 100 nm axial resolution. *J. Microsc.* **1999**, *195*, 10–16.
- (11) Ben-Levy, M.; Peleg, E. Imaging Measurement System. U.S. Patent USOO5867604A, 1999.
- (12) Heintzmann, R.; Cremer, C. Improvement of Transversal Resolution by Lateral Modulation. In *Abstracts of Papers, Focus on Microscopy*; 1999; p 24.
- (13) Cragg, G. E.; So, P. T. C. Lateral resolution enhancement with standing evanescent waves. *Opt. Lett.* **2000**, *25* (1), 46–48.
- (14) Frohn, J. T.; Knapp, H. F.; Stemmer, A. True optical resolution beyond the Rayleigh limit achieved by standing wave illumination. *Proc. Natl. Acad. Sci. U. S. A.* **2000**, *97* (13), 7232–7236.
- (15) Heintzmann, R. Saturated patterned excitation microscopy with two-dimensional excitation patterns. *Micron* **2003**, *34* (6–7), 283–291.
- (16) Gustafsson, M. G. L.; Agard, D. A.; Sedat, J. W. In *Three-Dimensional and Multidimensional Microscopy: Image Acquisition Processing VII*; Conchello, J.-A., Cogswell, C. J., Tescher, A. G., Wilson, T., Eds.; SPIE: 2000; Vol. 3919.
- (17) Fedossev, R.; Belyaev, Y.; Frohn, J.; Stemmer, A. Structured light illumination for extended resolution in fluorescence microscopy. *Opt. Laser Eng.* **2005**, *43* (3–5), 403–414.
- (18) Shao, L.; Isaac, B.; Uzawa, S.; Agard, D. A.; Sedat, J. W.; Gustafsson, M. G. L. I(S)S: Wide-field light microscopy with 100-nm-scale resolution in three dimensions. *Biophys. J.* **2008**, *94* (12), 4971–4983.
- (19) Fiolka, R.; Wicker, K.; Heintzmann, R.; Stemmer, A. Simplified approach to diffraction tomography in optical microscopy. *Opt. Express* **2009**, *17* (15), 12407–12417.
- (20) Hirvonen, L. M.; Wicker, K.; Mandula, O.; Heintzmann, R. Structured illumination microscopy of a living cell. *Eur. Biophys. J.* **2009**, *38* (6), 807–812.
- (21) Wicker, K.; Walde, M.; Oldewurtel, E. R.; Hirvonen, L.; Mandula, O.; Sindbert, S.; Heintzmann, R. Structured Illumination and Image Inversion Interferometry. *Biophys. J.* **2010**, *98* (3), 619a–619a.
- (22) Best, G.; Amberger, R.; Baddeley, D.; Ach, T.; Dithmar, S.; Heintzmann, R.; Cremer, C. Structured illumination microscopy of autofluorescent aggregations in human tissue. *Micron* **2011**, *42* (4), 330–335.
- (23) Heintzmann, R.; Jovin, T. M.; Cremer, C. Saturated patterned excitation microscopy - a concept for optical resolution improvement. *J. Opt. Soc. Am. A* **2002**, *19* (8), 1599–1609.
- (24) Heintzmann, R.; Cremer, C. German Patent DE 1990 8883 A1, 2000.
- (25) Hell, S. W.; Wichmann, J. Breaking the Diffraction Resolution Limit by Stimulated-Emission - Stimulated-Emission-Depletion Fluorescence Microscopy. *Opt. Lett.* **1994**, *19* (11), 780–782.
- (26) Klar, T. A.; Jakobs, S.; Dyba, M.; Egner, A.; Hell, S. W. Fluorescence microscopy with diffraction resolution barrier broken by stimulated emission. *Proc. Natl. Acad. Sci. U. S. A.* **2000**, *97* (15), 8206–8210.
- (27) Hofmann, M.; Eggeling, C.; Jakobs, S.; Hell, S. W. Breaking the diffraction barrier in fluorescence microscopy at low light intensities by

- using reversibly photoswitchable proteins. *Proc. Natl. Acad. Sci. U. S. A.* **2005**, *102* (49), 17565–17569.
- (28) Bouwhuis, G.; Spruit, J. H. M. Optical storage read-out of nonlinear disks. *Appl. Opt.* **1990**, *29*, 3766–3768.
- (29) So, P. T. C.; Kwon, H. S.; Dong, C. Y. Resolution enhancement in standing-wave total internal reflection microscopy: a point-spread-function engineering approach. *J. Opt. Soc. Am. A* **2001**, *18* (11), 2833–2845.
- (30) So, P. T. C.; Sutin, J. J.; Cragg, G. Biological imaging using Standing Wave Total Internal Reflection Microscopy. *Biophys. J.* **2001**, *80* (1), 165a–166a.
- (31) Chung, E.; Kim, D. K.; So, P. T. C. Extended resolution wide-field optical imaging: objective-launched standing-wave total internal reflection fluorescence microscopy. *Opt. Lett.* **2006**, *31* (7), 945–947.
- (32) Kner, P.; Chhun, B. B.; Griffis, E. R.; Winoto, L.; Gustafsson, M. G. L. Super-resolution video microscopy of live cells by structured illumination. *Nat. Methods* **2009**, *6* (5), 339–342.
- (33) Gustafsson, M. G. L.; Shao, L.; Carlton, P. M.; Wang, C. J. R.; Golubovskaya, I. N.; Cande, W. Z.; Agard, D. A.; Sedat, J. W. Three-dimensional resolution doubling in wide-field fluorescence microscopy by structured illumination. *Biophys. J.* **2008**, *94* (12), 4957–4970.
- (34) Gliko, O.; Brownell, W. E.; Saggau, P. Fast two-dimensional standing-wave total-internal-reflection fluorescence microscopy using acousto-optic deflectors. *Opt. Lett.* **2009**, *34* (6), 836–838.
- (35) Chakrova, N.; Heintzmann, R.; Rieger, B.; Stallinga, S. Studying different illumination patterns for resolution improvement in fluorescence microscopy. *Opt. Express* **2015**, *23* (24), 31367–31383.
- (36) Chen, B. C.; Legant, W. R.; Wang, K.; Shao, L.; Milkie, D. E.; Davidson, M. W.; Janetopoulos, C.; Wu, X. S.; Hammer, J. A., 3rd; Liu, Z.; et al. Lattice light-sheet microscopy: imaging molecules to embryos at high spatiotemporal resolution. *Science* **2014**, *346* (6208), 1257998.
- (37) Perez, V.; Chang, B. J.; Stelzer, E. H. Optimal 2D-SIM reconstruction by two filtering steps with Richardson-Lucy deconvolution. *Sci. Rep.* **2016**, *6*, 37149.
- (38) Chang, B. J.; Perez Meza, V. D.; Stelzer, E. H. K. csiLSFM combines light-sheet fluorescence microscopy and coherent structured illumination for a lateral resolution below 100 nm. *Proc. Natl. Acad. Sci. U. S. A.* **2017**, *114* (19), 4869–4874.
- (39) Planchon, T. A.; Gao, L.; Milkie, D. E.; Davidson, M. W.; Galbraith, J. A.; Galbraith, C. G.; Betzig, E. Rapid three-dimensional isotropic imaging of living cells using Bessel beam plane illumination. *Nat. Methods* **2011**, *8* (5), 417–423.
- (40) Thomas, B.; Momany, M.; Kner, P. Optical sectioning structured illumination microscopy with enhanced sensitivity. *J. Opt.* **2013**, *15* (9), 094004.
- (41) Thomas, B.; Wolstenholme, A.; Chaudhari, S. N.; Kipreos, E. T.; Kner, P. Enhanced resolution through thick tissue with structured illumination and adaptive optics. *J. Biomed. Opt.* **2015**, *20* (2), 026006.
- (42) Bruchez, M., Jr.; Moronne, M.; Gin, P.; Weiss, S.; Alivisatos, A. P. Semiconductor nanocrystals as fluorescent biological labels. *Science* **1998**, *281* (5385), 2013–2016.
- (43) Hsiao, W. W.; Hui, Y. Y.; Tsai, P. C.; Chang, H. C. Fluorescent Nanodiamond: A Versatile Tool for Long-Term Cell Tracking, Super-Resolution Imaging, and Nanoscale Temperature Sensing. *Acc. Chem. Res.* **2016**, *49* (3), 400–407.
- (44) Liu, Y.; Lu, Y.; Yang, X.; Zheng, X.; Wen, S.; Wang, F.; Vidal, X.; Zhao, J.; Liu, D.; Zhou, Z.; et al. Amplified stimulated emission in upconversion nanoparticles for super-resolution nanoscopy. *Nature* **2017**, *543*, 229–233.
- (45) Zhu, C.; Liu, L.; Yang, Q.; Lv, F.; Wang, S. Water-soluble conjugated polymers for imaging, diagnosis, and therapy. *Chem. Rev.* **2012**, *112* (8), 4687–4735.
- (46) Hennig, S.; Monkemoller, V.; Boger, C.; Muller, M.; Huser, T. Nanoparticles as Nonfluorescent Analogues of Fluorophores for Optical Nanoscopy. *ACS Nano* **2015**, *9* (6), 6196–6205.
- (47) Schnell, U.; Dijk, F.; Sjollema, K. A.; Giepmans, B. N. Immunolabeling artifacts and the need for live-cell imaging. *Nat. Methods* **2012**, *9* (2), 152–158.
- (48) Dale, B. M.; McNerney, G. P.; Thompson, D. L.; Hubner, W.; de los Reyes, K.; Chuang, F. Y. S.; Huser, T.; Chen, B. K. Cell-to-Cell Transfer of HIV-1 via Virological Synapses Leads to Endosomal Virion Maturation that Activates Viral Membrane Fusion. *Cell Host Microbe* **2011**, *10* (6), 551–562.
- (49) Rego, E. H.; Shao, L.; Macklin, J. J.; Winoto, L.; Johansson, G. A.; Kamps-Hughes, N.; Davidson, M. W.; Gustafsson, M. G. L. Nonlinear structured-illumination microscopy with a photoswitchable protein reveals cellular structures at 50-nm resolution. *Proc. Natl. Acad. Sci. U. S. A.* **2012**, *109* (3), E135–E143.
- (50) Li, D.; Shao, L.; Chen, B. C.; Zhang, X.; Zhang, M. S.; Moses, B.; Milkie, D. E.; Beach, J. R.; Hammer, J. A.; Pasham, M.; et al. Extended-resolution structured illumination imaging of endocytic and cytoskeletal dynamics. *Science* **2015**, *349* (6251), aab3500.
- (51) Lu-Walther, H. W.; Hou, W.; Kielhorn, M.; Arai, Y.; Nagai, T.; Kessels, M. M.; Qualmann, B.; Heintzmann, R. Nonlinear Structured Illumination Using a Fluorescent Protein Activating at the Readout Wavelength. *PLoS One* **2016**, *11* (10), e0165148.
- (52) Wicker, K.; Mandula, O.; Best, G.; Fiolka, R.; Heintzmann, R. Phase optimization for structured illumination microscopy. *Opt. Express* **2013**, *21* (2), 2032–2049.
- (53) O'Holleran, K.; Shaw, M. Optimized approaches for optical sectioning and resolution enhancement in 2D structured illumination microscopy. *Biomed. Opt. Express* **2014**, *5* (8), 2580–2590.
- (54) Lal, A.; Shan, C. Y.; Xi, P. Structured Illumination Microscopy Image Reconstruction Algorithm. *IEEE J. Sel. Top. Quantum Electron.* **2016**, *22* (4), 6803414.
- (55) Krizek, P.; Lukes, T.; Ovesny, M.; Fliegel, K.; Hagen, G. M. SIMToolbox: a MATLAB toolbox for structured illumination fluorescence microscopy. *Bioinformatics* **2016**, *32* (2), 318–320.
- (56) Muller, M.; Monkemoller, V.; Hennig, S.; Hubner, W.; Huser, T. Open-source image reconstruction of super-resolution structured illumination microscopy data in ImageJ. *Nat. Commun.* **2016**, *7*, 10980.
- (57) Schneider, C. A.; Rasband, W. S.; Eliceiri, K. W. NIH Image to ImageJ: 25 years of image analysis. *Nat. Methods* **2012**, *9* (7), 671–675.
- (58) Ball, G.; Demmerle, J.; Kaufmann, R.; Davis, I.; Dobbie, I. M.; Schermelleh, L. SIMcheck: a Toolbox for Successful Super-resolution Structured Illumination Microscopy. *Sci. Rep.* **2015**, *5*, 15915.
- (59) Negash, A.; Labouesse, S.; Sandeau, N.; Allain, M.; Giovannini, H.; Idier, J.; Heintzmann, R.; Chaumet, P. C.; Belkebir, K.; Sentenac, A. Improving the axial and lateral resolution of three-dimensional fluorescence microscopy using random speckle illuminations. *J. Opt. Soc. Am. A* **2016**, *33* (6), 1089–1094.
- (60) Jost, A.; Tolstik, E.; Feldmann, P.; Wicker, K.; Sentenac, A.; Heintzmann, R. Optical Sectioning and High Resolution in Single-Slice Structured Illumination Microscopy by Thick Slice Blind-SIM Reconstruction. *PLoS One* **2015**, *10* (7), e0132174.
- (61) Sheppard, C. J. R. Super-resolution in confocal imaging. *Optik (Stuttgart, Ger.)* **1988**, *80* (2), 53–54.
- (62) Müller, C. B.; Enderlein, J. Image Scanning Microscopy. *Phys. Rev. Lett.* **2010**, *104* (19), 198101.
- (63) York, A. G.; Parekh, S. H.; Nogare, D. D.; Fischer, R. S.; Temprine, K.; Mione, M.; Chitnis, A. B.; Combs, C. A.; Shroff, H. Resolution doubling in live, multicellular organisms via multifocal structured illumination microscopy. *Nat. Methods* **2012**, *9* (7), 749–754.
- (64) Schulz, O.; Pieper, C.; Clever, M.; Pfaff, J.; Ruhlandt, A.; Kehlenbach, R. H.; Wouters, F. S.; Grosshans, J.; Bunt, G.; Enderlein, J. Resolution doubling in fluorescence microscopy with confocal spinning-disk image scanning microscopy. *Proc. Natl. Acad. Sci. U. S. A.* **2013**, *110* (52), 21000–21005.
- (65) Azuma, T.; Kei, T. Super-resolution spinning-disk confocal microscopy using optical photon reassignment. *Opt. Express* **2015**, *23* (11), 15003–15011.
- (66) Ingaramo, M.; York, A. G.; Wawrzusin, P.; Milberg, O.; Hong, A.; Weigert, R.; Shroff, H.; Patterson, G. H. Two-photon excitation improves multifocal structured illumination microscopy in thick

- scattering tissue. *Proc. Natl. Acad. Sci. U. S. A.* **2014**, *111* (14), 5254–5259.
- (67) Roth, S.; Sheppard, C. J. R.; Wicker, K.; Heintzmann, R. Optical photon reassignment microscopy (OPRA). *Opt. Nanosc.* **2013**, *2* (1), 5.
- (68) Sheppard, C. J. R.; Mehta, S. B.; Heintzmann, R. Super-resolution by image scanning microscopy using pixel reassignment. *Opt. Lett.* **2013**, *38* (15), 2889–2892.
- (69) De Luca, G. M.; Breedijk, R. M.; Brandt, R. A.; Zeelenberg, C. H.; de Jong, B. E.; Timmermans, W.; Azar, L. N.; Hoebe, R. A.; Stallinga, S.; Manders, E. M. Re-scan confocal microscopy: scanning twice for better resolution. *Biomed. Opt. Express* **2013**, *4* (11), 2644–2656.
- (70) York, A. G.; Chandris, P.; Nogare, D. D.; Head, J.; Wawrzusin, P.; Fischer, R. S.; Chitnis, A.; Shroff, H. Instant super-resolution imaging in live cells and embryos via analog image processing. *Nat. Methods* **2013**, *10* (11), 1122–1126.
- (71) Winter, P. W.; York, A. G.; Nogare, D. D.; Ingaramo, M.; Christensen, R.; Chitnis, A.; Patterson, G. H.; Shroff, H. Two-photon instant structured illumination microscopy improves the depth penetration of super-resolution imaging in thick scattering samples. *Optica* **2014**, *1* (3), 181–191.
- (72) Rossberger, S.; Best, G.; Baddeley, D.; Heintzmann, R.; Birk, U.; Dithmar, S.; Cremer, C. Combination of structured illumination and single molecule localization microscopy in one setup. *J. Opt.* **2013**, *15* (9), 094003.
- (73) Mönkemöller, V.; Øie, C.; Hübner, W.; Huser, T.; McCourt, P. Multimodal super-resolution optical microscopy visualizes the close connection between membrane and the cytoskeleton in liver sinusoidal endothelial cell fenestrations. *Sci. Rep.* **2015**, *5*, 16279.
- (74) Masip, M. E.; Huebinger, J.; Christmann, J.; Sabet, O.; Wehner, F.; Konitsiotis, A.; Fuhr, G. R.; Bastiaens, P. I. Reversible cryo-arrest for imaging molecules in living cells at high spatial resolution. *Nat. Methods* **2016**, *13* (8), 665–672.
- (75) Gustafsson, M. G. L. Nonlinear structured-illumination microscopy: Wide-field fluorescence imaging with theoretically unlimited resolution. *Proc. Natl. Acad. Sci. U. S. A.* **2005**, *102* (37), 13081–13086.
- (76) Andresen, M.; Stiel, A. C.; Folling, J.; Wenzel, D.; Schonle, A.; Egner, A.; Eggeling, C.; Hell, S. W.; Jakobs, S. Photoswitchable fluorescent proteins enable monochromatic multilabel imaging and dual color fluorescence nanoscopy. *Nat. Biotechnol.* **2008**, *26* (9), 1035–1040.
- (77) Schermelleh, L.; Carlton, P. M.; Haase, S.; Shao, L.; Winoto, L.; Kner, P.; Burke, B.; Cardoso, M. C.; Agard, D. A.; Gustafsson, M. G. L.; et al. Subdiffraction multicolor imaging of the nuclear periphery with 3D structured illumination microscopy. *Science* **2008**, *320* (5881), 1332–1336.
- (78) Wang, C. J. R.; Carlton, P. M.; Golubovskaya, I. N.; Cande, W. Z. Interlock Formation and Coiling of Meiotic Chromosome Axes During Synapsis. *Genetics* **2009**, *183* (3), 905–915.
- (79) Sonnen, K. F.; Schermelleh, L.; Leonhardt, H.; Nigg, E. A. 3D-structured illumination microscopy provides novel insight into architecture of human centrosomes. *Biol. Open* **2012**, *1* (10), 965–976.
- (80) Chagin, V. O.; Casas-Delucchi, C. S.; Reinhart, M.; Schermelleh, L.; Markaki, Y.; Maiser, A.; Bolius, J. J.; Bensimon, A.; Fillies, M.; Domaing, P.; et al. 4D Visualization of replication foci in mammalian cells corresponding to individual replicons. *Nat. Commun.* **2016**, *7*, 11231.
- (81) Brown, A. C.; Oddos, S.; Dobbie, I. M.; Alakoskela, J. M.; Parton, R. M.; Eissmann, P.; Neil, M. A.; Dunsby, C.; French, P. M.; Davis, I.; et al. Remodelling of cortical actin where lytic granules dock at natural killer cell immune synapses revealed by super-resolution microscopy. *PLoS Biol.* **2011**, *9* (9), e1001152.
- (82) Cogger, V. C.; McNerney, G. P.; Nyunt, T.; DeLeve, L. D.; McCourt, P.; Smedsrod, B.; Le Couteur, D. G.; Huser, T. R. Three-dimensional structured illumination microscopy of liver sinusoidal endothelial cell fenestrations. *J. Struct. Biol.* **2010**, *171* (3), 382–388.
- (83) Regev-Rudzki, N.; Wilson, D. W.; Carvalho, T. G.; Sisquella, X.; Coleman, B. M.; Rug, M.; Bursac, D.; Angrisano, F.; Gee, M.; Hill, A. F.; et al. Cell-cell communication between malaria-infected red blood cells via exosome-like vesicles. *Cell* **2013**, *153* (5), 1120–1133.
- (84) Riglar, D. T.; Rogers, K. L.; Hanssen, E.; Turnbull, L.; Bullen, H. E.; Charnaud, S. C.; Przyborski, J.; Gilson, P. R.; Whitchurch, C. B.; Crabb, B. S.; et al. Spatial association with PTEX complexes defines regions for effector export into Plasmodium falciparum-infected erythrocytes. *Nat. Commun.* **2013**, *4*, 1415.
- (85) Strauss, M. P.; Liew, A. T.; Turnbull, L.; Whitchurch, C. B.; Monahan, L. G.; Harry, E. J. 3D-SIM super resolution microscopy reveals a bead-like arrangement for FtsZ and the division machinery: implications for triggering cytokinesis. *PLoS Biol.* **2012**, *10* (9), e1001389.
- (86) Rowlett, V. W.; Margolin, W. 3D-SIM super-resolution of FtsZ and its membrane tethers in Escherichia coli cells. *Biophys. J.* **2014**, *107* (8), L17–L20.
- (87) Lesterlin, C.; Ball, G.; Schermelleh, L.; Sherratt, D. J. RecA bundles mediate homology pairing between distant sisters during DNA break repair. *Nature* **2014**, *506* (7487), 249–253.
- (88) Bisson-Filho, A. W.; Hsu, Y. P.; Squyres, G. R.; Kuru, E.; Wu, F. B.; Jukes, C.; Sun, Y. J.; Dekker, C.; Holden, S.; VanNieuwenhze, M. S.; et al. Treadmilling by FtsZ filaments drives peptidoglycan synthesis and bacterial cell division. *Science* **2017**, *355* (6326), 739–743.
- (89) Horsington, J.; Turnbull, L.; Whitchurch, C. B.; Newsome, T. P. Sub-viral imaging of vaccinia virus using super-resolution microscopy. *J. Virol. Methods* **2012**, *186* (1–2), 132–136.
- (90) Fitzgibbon, J.; Bell, K.; King, E.; Oparka, K. Super-resolution imaging of plasmodesmata using three-dimensional structured illumination microscopy. *Plant Physiol.* **2010**, *153* (4), 1453–1463.
- (91) Tilsner, J.; Linnik, O.; Louveaux, M.; Roberts, I. M.; Chapman, S. N.; Oparka, K. J. Replication and trafficking of a plant virus are coupled at the entrances of plasmodesmata. *J. Cell Biol.* **2013**, *201* (7), 981–995.
- (92) Linnik, O.; Liesche, J.; Tilsner, J.; Oparka, K. J. Unraveling the structure of viral replication complexes at super-resolution. *Front. Plant Sci.* **2013**, *4*, 6.
- (93) Wanner, G.; Schroeder-Reiter, E.; Ma, W.; Houben, A.; Schubert, V. The ultrastructure of mono- and holocentric plant centromeres: an immunological investigation by structured illumination microscopy and scanning electron microscopy. *Chromosoma* **2015**, *124* (4), 503–517.
- (94) Schubert, V.; Weisshart, K. Abundance and distribution of RNA polymerase II in Arabidopsis interphase nuclei. *J. Exp. Bot.* **2015**, *66* (6), 1687–1698.
- (95) Shao, L.; Kner, P.; Rego, E. H.; Gustafsson, M. G. L. Super-resolution 3D microscopy of live whole cells using structured illumination. *Nat. Methods* **2011**, *8* (12), 1044–1046.
- (96) Fiolka, R.; Shao, L.; Rego, E. H.; Davidson, M. W.; Gustafsson, M. G. L. Time-lapse two-color 3D imaging of live cells with doubled resolution using structured illumination. *Proc. Natl. Acad. Sci. U. S. A.* **2012**, *109* (14), 5311–5315.
- (97) Lu-Walther, H. W.; Kielhorn, M.; Forster, R.; Jost, A.; Wicker, K.; Heintzmann, R. fastSIM: a practical implementation of fast structured illumination microscopy. *Methods Appl. Fluoresc.* **2015**, *3* (1), 014001.
- (98) Song, L. Y.; Lu-Walther, H. W.; Forster, R.; Jost, A.; Kielhorn, M.; Zhou, J. Y.; Heintzmann, R. Fast structured illumination microscopy using rolling shutter cameras. *Meas. Sci. Technol.* **2016**, *27* (5), 055401.
- (99) Sahl, S. J.; Balzarotti, F.; Keller-Findeisen, J.; Leutenegger, M.; Westphal, V.; Egner, A.; Lavoie-Cardinal, F.; Chmyrov, A.; Grotjohann, T.; Jakobs, S. Comment on “Extended-resolution structured illumination imaging of endocytic and cytoskeletal dynamics”. *Science* **2016**, *352* (6285), 527.
- (100) Li, D.; Betzig, E. Response to Comment on “Extended-resolution structured illumination imaging of endocytic and cytoskeletal dynamics”. *Science* **2016**, *352* (6285), 527.

- (101) Nixon-Abell, J.; Obara, C. J.; Weigel, A. V.; Li, D.; Legant, W. R.; Xu, C. S.; Pasolli, H. A.; Harvey, K.; Hess, H. F.; Betzig, E.; et al. Increased spatiotemporal resolution reveals highly dynamic dense tubular matrices in the peripheral ER. *Science* **2016**, *354* (6311), aaf3928.
- (102) Abrahamsson, S.; Blom, H.; Agostinho, A.; Jans, D. C.; Jost, A.; Muller, M.; Nilsson, L.; Bernhem, K.; Lambert, T. J.; Heintzmann, R.; et al. Multifocus structured illumination microscopy for fast volumetric super-resolution imaging. *Biomed. Opt. Express* **2017**, *8* (9), 4135–4140.
- (103) Hell, S. W.; Sahl, S. J.; Bates, M.; Zhuang, X. W.; Heintzmann, R.; Booth, M. J.; Bewersdorf, J.; Shtengel, G.; Hess, H.; Tinnefeld, P.; et al. The 2015 super-resolution microscopy roadmap. *J. Phys. D: Appl. Phys.* **2015**, *48* (44), 443001.
- (104) Mo, G. C. H.; Ross, B.; Hertel, F.; Manna, P.; Yang, X. X.; Greenwald, E.; Booth, C.; Plummer, A. M.; Tenner, B.; Chen, Z.; et al. Genetically encoded biosensors for visualizing live-cell biochemical activity at super-resolution. *Nat. Methods* **2017**, *14* (4), 427–434.